THERMAL DESIGN OPTIMIZATION OF MULTI-PASSAGE INTERNALLY COOLED TURBINE BLADES

by

JAMES D. RUIZ

Presented to the Faculty of the Graduate School of

The University of Texas at Arlington in Partial Fulfillment

of the Requirements for the Degree of

MASTER OF SCIENCE IN AEROSPACE ENGINEERING

THE UNIVERSITY OF TEXAS AT ARLINGTON

December 2008

ACKNOWLEDGEMENTS

To start I would like to thank the individuals who, in some form, have contributed to my work and success here at UT-Arlington. Starting with my classmates: Weiya, Harsh, Takahiro, La, Katie and Rajeev. Thank you for sharing your knowledge and opinions. To my professor, Dr. Brian Dennis, thank you for working with me to make this project a success and thank you for working with me during my transition.

To my personal friends: Chinmay Adhvaryu, thank you for the assistance you provided, no matter where in the United States you or I may have been. Your help has been greatly appreciated and your friendship even more valuable. To Marisa Guzman, thank you for your endless support. This journey has been one that we have contributed to together and can now enjoy our accomplishment.

November 25, 2008

ABSTRACT

THERMAL DESIGN OPTIMIZATION OF MULTI-PASSAGE
INTERNALLY COOLED TURBINE BLADES

James D. Ruiz, M.S.

The University of Texas at Arlington, 2008

Supervising Professor: Brian H. Dennis

This paper outlines the use of Computational Fluid Dynamics (CFD) and Genetic Algorithm (GA) Optimization to enhance the design of a 3-dimensional internally cooled turbine blade. The optimization code utilizes principles of Genetic Algorithms to optimize (i.e. minimize) the integrated heat flux through the turbine blade. The optimization is accomplished by adjusting the size and position (within pre-determined constraints) of cooling passages internal to the turbine blade. Starting with an aerodynamically optimized airfoil shape, cooling passage designs are generated by the optimization process and coupled with boundary and airfoil domains. The analysis becomes a Conjugate Heat Transfer (CHT) problem analyzing convective heat transfer between the hot gas boundary and the solid airfoil, thermal conduction within the airfoil and convective heat transfer between the solid airfoil and cold gas flow. The turbine blade is analyzed aerodynamically and thermodynamically using FLUENT CFD software. The analysis process is fully automated to produce thermodynamic results of the turbine blade design. Solution of the CHT problem is output as integrated heat flux over the blade surface and maximum temperature within the turbine blade. These values are transferred back to the optimization code as quantities of interest for the optimizer.

The optimization code and CFD analysis work iteratively until convergence is achieved through minimized heat flux while maintaining a maximum allowable temperature within the airfoil. Aerodynamic and thermal solutions for the initial airfoil and final airfoil geometry are presented.

TABLE OF CONTENTS

LIST OF ILLUSTRATIONS

LIST OF TABLES

CHAPTER 1

INTRODUCTION

The present thesis investigates the use of commercial CFD codes along with a Genetic Algorithm Optimization code to optimize the design of internally cooled turbine blade. Current design turbines inlet temperatures can be on the order of 1800K. The turbine inlet temperatures can often exceed the thermal capacity of the turbine blade materials. Three ways of combating this problem are: 1) advancement of blade materials to withstand such operating temperatures, 2) reduction of the engine performance (i.e. fuel-to-air-ratio) which will effectively reduce the turbine inlet temperatures, and 3) cooling of the turbine blades to allow current materials to withstand higher than normal operating temperatures. This paper will focus on the third option of internal blade cooling.

Blade cooling is accomplished by routing relatively cool air from the engine compressor section to the turbine (rotating) or stator (non-rotating) blades. The method utilized in this analysis uses circular cooling passages that maintain a constant diameter along the length of a constant shape airfoil. The reason for this approach is to simplify the process for proof of concept and for comparison to similar published experimental data.

1.1 Content of Thesis

Chapter 2 of this thesis introduces the governing equations behind CFD as they apply to the analysis of a turbine blade. It also outlines the numerical method and discretization schemes associated with the aforementioned analysis. A description of FLUENT CFD software and GAMBIT Grid Generation software are presented. In addition, chapter 2 contains some validation work completed on experimental cases using FLUENT CFD software.

Chapter 3 summarizes the theory behind Genetic Algorithms and their function in this analysis.

Chapter 4 outlines the steps used in the optimization/analysis process as they link the functions between the GA Optimization code, Gambit, Fluent and intermediate processes in the analysis sequence. Contained within chapter 4 is the setup of the analysis, the analysis model and test parameters.

Chapter 5 discusses the results of the model geometry prior to cooling, with the initial cooling design and the final optimized design. The results detail thermodynamic parameters at each point and the proof of concept for turbine cooling optimization.

CHAPTER 2

INTRODUCTION TO COMPUTATIONAL FLUID DYNAMICS

Computational Fluid Dynamics, commonly referred to as CFD, is defined as the set of methodologies that enable the computer to provide us with a numerical simulation of fluid flows. We use the word simulation to indicate that we use the computer to solve numerically the laws that govern the movements of fluids, in or around material system. CFD begins with the definition of equations that govern fluid flow. These equations are partial differential equations govern the conservation of mass flow, momentum flow and energy flow through a medium (i.e. solid, gas or liquid). Once defined, the governing equations are applied to a discretized fluid or solid domain. A discretized domain is an area or volume of interest that is broken up into smaller areas or volumes over which the governing equations are applied. The governing equations are applied to each control volume in 3D (or area in 2D) of interest using the Finite Volume Method.

2.1 Governing Equations

The governing equations used in CFD are a culmination of numerical and empirical equations derived to adequately depict the nature of fluid flow. The type and quantity of equations used in the numerical analysis of a model depend on the type of flow conditions experienced and the type of engineering quantities evaluated. In the model of an internally cooled turbine blade, engineering quantities such as velocity, pressure and temperature are evaluated as well as turbulence quantities that affect the fluid flow. Therefore, governing equations in this analysis must consist of fluid flow, energy and turbulence models to adequately define the flow characteristics. Below is a description of equations used in the numerical analysis and an explanation of how each equation is applied. A derivation of the equation will not be included but can be referenced in the references section of this report

2.1.1 Conservation of Mass

Mass conservation is based on the theory that mass can neither be created nor destroyed. Applying mass conservation laws to a 3-dimensional control volume, the following conservation equation for 3-dimensional, unsteady and compressible flow are derived by Tu et al [2].

$$\frac{\partial \rho}{\partial t} + \frac{\partial u\rho}{\partial x} + \frac{\partial v\rho}{\partial y} + \frac{\partial w\rho}{\partial x} = 0 \qquad 2.1$$

The flow conditions of the turbine blade analysis dictate that the flow will modeled as compressible since the hot gas Mach number will be on the order of 0.8 which exceeds the maximum suggested Mach number for incompressible flows of 0.3. A steady state flow analysis is conducted since transient effects of the fluid flow have no effect on the final solution. Therefore, the first term in equation 2.1 can be set equal to zero.

$$\frac{\partial \rho}{\partial t} = 0 \qquad \frac{k}{\varepsilon}\frac{\partial \bar{u}}{\partial x} \geq \frac{1}{3C_{\mu}} = 0 \qquad 2.2$$

2.1.2 Momentum: Force Balance

Momentum equations are derived from Newton's Second Law of Motion that states that forces on a fluid volume must be balanced. From here the derived equations for momentum on a fluid volume are listed below. These equations dictate the transfer of momentum through a 3-dimensional, compressible, unsteady Newtonian field.

$$\frac{\partial \rho u}{\partial t} + \frac{\partial \rho uu}{\partial x} + \frac{\partial \rho vu}{\partial y} + \frac{\partial \rho wu}{\partial z} = -\frac{\partial p}{\partial x} + \mu\frac{\partial^2 u}{\partial x^2} + \mu\frac{\partial^2 u}{\partial y^2} + \mu\frac{\partial^2 u}{\partial z^2} + S_x \qquad 2.3$$

$$\frac{\partial \rho v}{\partial t} + \frac{\partial \rho uv}{\partial x} + \frac{\partial \rho vv}{\partial y} + \frac{\partial \rho wv}{\partial z} = -\frac{\partial p}{\partial y} + \mu\frac{\partial^2 v}{\partial x^2} + \mu\frac{\partial^2 v}{\partial y^2} + \mu\frac{\partial^2 v}{\partial z^2} + S_y \qquad 2.4$$

$$\frac{\partial \rho w}{\partial t} + \frac{\partial \rho uw}{\partial x} + \frac{\partial \rho vw}{\partial y} + \frac{\partial \rho ww}{\partial z} = -\frac{\partial p}{\partial z} + \mu\frac{\partial^2 w}{\partial x^2} + \mu\frac{\partial^2 w}{\partial y^2} + \mu\frac{\partial^2 w}{\partial z^2} + S_z \qquad 2.5$$

The momentum equations contain the local dynamic viscosity (μ) which is defined for the fluid at the inlet. Since we are conducting steady state analysis the local acceleration terms are neglected.

$$\frac{\partial \rho u}{\partial t} = \frac{\partial \rho v}{\partial t} = \frac{\partial \rho w}{\partial t} = 0$$

2.1.3 Conservation of Energy

Derived from the First Law of Thermodynamics, the energy equation states that the time rate change of energy within a control volume must equal the net rate of heat added to the system plus the net rate of work done on the system. Applying this law to a 3-dimensional control volume and using Fourier's law of heat conduction the 3-dimensional energy conservation equation (2.6) is derived by Tu et al [2].

$$\frac{\partial T}{\partial t} + \frac{\partial uT}{\partial x} + \frac{\partial vT}{\partial y} + \frac{\partial wT}{\partial z} = \frac{k}{\rho C_p}\left[\frac{\partial^2 T}{\partial x^2} + \frac{\partial^2 T}{\partial y^2} + \frac{\partial^2 T}{\partial z^2}\right] + \frac{1}{\rho C_p}\frac{\partial p}{\partial t} + \frac{\Phi}{\rho C_p} \qquad 2.6$$

The effects on energy due to viscous stresses are represented by the dissipation function (Φ).This source of energy is due to mechanical work on the fluid that is converted into energy. Using Newton's Law of viscosity, the shear stresses on the control volume are can be converted into velocity gradients and therefore the dissipation function is expressed as:

$$\Phi = \left(\frac{\partial u\tau_{xx}}{\partial x}\right) + \left(\frac{\partial v\tau_{yx}}{\partial y}\right) + \left(\frac{\partial w\tau_{zx}}{\partial z}\right) + \left(\frac{\partial v\tau_{xy}}{\partial x}\right) + \left(\frac{\partial v\tau_{yy}}{\partial y}\right) + \left(\frac{\partial v\tau_{zx}}{\partial z}\right) + \left(\frac{\partial w\tau_{xz}}{\partial x}\right) + \left(\frac{\partial w\tau_{yz}}{\partial y}\right) + \left(\frac{\partial w\tau_{zz}}{\partial z}\right) \qquad 2.7$$

Similar to the mass and momentum conservation equations, the steady state analysis neglects the local acceleration of temperature.

$$\frac{\partial T}{\partial t} = 0$$

2.1.4 Turbulence

Turbulence is a fundamental aspect of most engineering problems in CFD. Turbulence describes the random and chaotic motion of viscous fluid flow. Turbulent flow can be visualized by rotational motion commonly referred to as turbulent eddies. Turbulent eddies, or rotational motion of the flow, are defined over a wide range of length scales. Length scales represent the size of turbulent eddies and are dependent on the size of the model and Reynolds number. Turbulent eddies relate to higher values of diffusion for mass, momentum and heat. In the case of turbine blade analysis, turbulent eddies can effect the rate of heat transfer from the free stream to the blade and can help prevent separation. The turbulence model utilized in this analysis is the two equation k-Epsilon model. This model is utilized for its proven accuracy in turbine blade analysis and for its applicability to confined fluid flow. Turbulent (random) fluctuations of fluid flow at any given point can be approximated by the time averaged component ($\bar{u}$) and the time fluctuating component ($u'(t)$): $u(t) = \bar{u} + u'(t)$. Similarly, mean values $\bar{v}$, $\bar{w}$, $\bar{p}$ and $\bar{T}$ and fluctuating components v', w', p' and T' are defined. From these approximations we must reconstruct our conservation equations to account for the time averaged and fluctuating values.

$$\frac{\partial \rho \overline{uu}}{\partial x} + \frac{\partial \rho \overline{vu}}{\partial y} + \frac{\partial \rho \overline{wu}}{\partial z} = -\frac{\partial \bar{p}}{\partial x} + \frac{\partial}{\partial x}\left[\nu \frac{\partial \bar{u}}{\partial x}\right] + \frac{\partial}{\partial y}\left[\nu \frac{\partial \bar{u}}{\partial y}\right] + \frac{\partial}{\partial z}\left[\nu \frac{\partial \bar{u}}{\partial z}\right] + Stresses + S_x \quad 2.8$$

$$\frac{\partial \rho \overline{uv}}{\partial x} + \frac{\partial \rho \overline{vv}}{\partial y} + \frac{\partial \rho \overline{wv}}{\partial z} = -\frac{\partial \bar{p}}{\partial y} + \frac{\partial}{\partial x}\left[\nu \frac{\partial \bar{v}}{\partial x}\right] + \frac{\partial}{\partial y}\left[\nu \frac{\partial \bar{v}}{\partial y}\right] + \frac{\partial}{\partial z}\left[\nu \frac{\partial \bar{v}}{\partial z}\right] + Stresses + S_y \quad 2.9$$

$$\frac{\partial \rho \overline{uw}}{\partial x} + \frac{\partial \rho \overline{vw}}{\partial y} + \frac{\partial \rho \overline{ww}}{\partial z} = -\frac{\partial \bar{p}}{\partial z} + \frac{\partial}{\partial x}\left[\nu \frac{\partial \bar{w}}{\partial x}\right] + \frac{\partial}{\partial y}\left[\nu \frac{\partial \bar{w}}{\partial y}\right] + \frac{\partial}{\partial z}\left[\nu \frac{\partial \bar{w}}{\partial z}\right] + Stresses + S_z \quad 2.10$$

$$\frac{\partial \overline{u}\overline{T}}{\partial x} + \frac{\partial \overline{v}\overline{T}}{\partial y} + \frac{\partial \overline{w}\overline{T}}{\partial z} = \frac{\partial}{\partial x}\left[\frac{\nu}{\mathrm{Pr}}\frac{\partial \bar{T}}{\partial x}\right] + \frac{\partial}{\partial y}\left[\frac{\nu}{\mathrm{Pr}}\frac{\partial \bar{T}}{\partial y}\right] + \frac{\partial}{\partial z}\left[\frac{\nu}{\mathrm{Pr}}\frac{\partial \bar{T}}{\partial z}\right] - \frac{1}{\rho}\left[\frac{\partial \overline{u'T'}}{\partial x} + \frac{\partial \overline{u'T'}}{\partial y} + \frac{\partial \overline{u'T'}}{\partial z}\right] + S_T \quad 2.11$$

The resulting conservation equations are commonly referred to as the Reynolds Averaged Navier Stokes Equations (RANS). The “S” terms in the RANS equations represent source terms due to gravity or other source that affect flow and temperature. The RANS equations are similar to the laminar Navier Stokes equations with the formulation of nine additional terms in three dimensions, for the momentum equations. The nine additional momentum terms are referred to as the Reynolds stresses and are listed in equations 2.8. It was formulated by Boussinesq (1868) that the Reynolds stresses can be linked to the average rates of deformation as follows:

$$Stresses = \begin{cases} \overline{u'u'} = -2\nu_T \dfrac{\partial \bar{u}}{\partial x} + \dfrac{2}{3}k \\ \overline{v'v'} = -2\nu_T \dfrac{\partial \bar{v}}{\partial y} + \dfrac{2}{3}k \\ \overline{w'w'} = -2\nu_T \dfrac{\partial \bar{w}}{\partial z} + \dfrac{2}{3}k \\ \overline{u'v'} = -\nu_T \left(\dfrac{\partial \bar{v}}{\partial x} + \dfrac{\partial \bar{u}}{\partial y} \right) \\ \overline{u'w'} = -\nu_T \left(\dfrac{\partial \bar{x}}{\partial z} + \dfrac{\partial \bar{w}}{\partial x} \right) \\ \overline{v'w'} = -\nu_T \left(\dfrac{\partial \bar{v}}{\partial z} + \dfrac{\partial \bar{w}}{\partial y} \right) \end{cases} for \begin{cases} x \\ y \\ z \\ x, y \\ x, z \\ y, z \end{cases} \qquad 2.12$$

For high Reynolds number flows, the normal strains in the normal stress equations become large. When the normal strains become large enough to satisfy following inequality, the normal stresses become negative which results in an unrealistic negative stress term. For a constant C_μ term, this inequality is approximately 3.7. The Realizable k-epsilon turbulence model remedies this situation by sensitizing C_μ to turbulent kinetic energy (k), turbulent dissipation (ε) and mean velocity. The formulation for C_μ can be found in FLUENT User’s Guid [8].

$$\frac{k}{\varepsilon}\frac{\partial \bar{u}}{\partial x} \geq \frac{1}{3C_\mu} \xrightarrow{C_\mu = 0.09} 3.7 \qquad 2.13$$

Two additional terms appear in the Reynolds stresses that represent turbulent viscosity (ν_T) and turbulent kinetic energy (k). Turbulent viscosity is computed locally from local turbulent kinetic energy and turbulent dissipation (ε) values.

$$\nu_T = \frac{\mu_T}{\rho} = \frac{C_\mu k^2}{\varepsilon} \qquad 2.14$$

The local turbulent kinetic energy is computed by equation 2.15. The kinetic energy is computed at the inlet from the specified turbulence intensity and the velocity by equation 2.16.

$$k_{local} = \frac{1}{2}(u'^2 + v'^2 + w'^2) \qquad 2.15$$

$$k_{inlet} = \frac{3}{2}\left[\frac{1}{3}\frac{(u'^2 + v'^2 + w'^2)}{(U^2 + V^2 + W^2)}\right](U^2 + V^2 + W^2) = \frac{3}{2}I^2V^2 \qquad 2.16$$

The turbulence intensity (I) is typically specified for turbine blade experiments and represents the ratio of root-mean-square of the turbulent fluctuations to the mean velocity. The turbulence intensity for high-turbulence flows in typically in the high 6%-20% range; however, for the experimental cases in this report the turbulent intensities are in the medium 1%-6% range. The turbulence intensity can also be approximated from Reynolds Number if direct measurements are not available.

$$I \approx 0.16\,\mathrm{Re}^{-1/8} \qquad 2.17$$

The turbulence dissipation is computed from the fluctuating velocity terms. At the inlet, the turbulence is defined by turbulent kinetic energy and the Turbulence Viscosity Ratio (TVR).

$$\varepsilon_{local} = \nu\left[\left(\frac{\partial u'}{\partial x}\right)^2 + \left(\frac{\partial v'}{\partial x}\right)^2 + \left(\frac{\partial w'}{\partial x}\right)^2 + \left(\frac{\partial u'}{\partial y}\right)^2 + \left(\frac{\partial v'}{\partial y}\right)^2 + \left(\frac{\partial w'}{\partial y}\right)^2 + \left(\frac{\partial u'}{\partial z}\right)^2 + \left(\frac{\partial v'}{\partial z}\right)^2 + \left(\frac{\partial w'}{\partial z}\right)^2\right] \qquad 2.18$$

$$\varepsilon_{inlet} = \frac{0.09k^2}{TVR\,\nu} \qquad 2.19$$

For inlet Reynolds numbers greater than 100,000, the TVR is empirically stated to be approximately 100. Other methods for specifying turbulence dissipation include length scale and hydraulic diameter. The equations for these methods vary from what is presented here.

In the energy equation the fluctuating temperature and velocity terms are related to the gradient of the mean temperature by equations 2.20. These equations are formulated in terms of Turbulent Prandtl number (Pr_T) and turbulent viscosity. Based on experimental data [1], the Turbulent Prandtl number is equal to unity.

$$\overline{u'T'} = -\frac{\mu_T}{\rho \mathrm{Pr}_T}\frac{\partial \overline{T}}{\partial x} \qquad \overline{v'T'} = -\frac{\mu_T}{\rho \mathrm{Pr}_T}\frac{\partial \overline{T}}{\partial y} \qquad \overline{w'T'} = -\frac{\mu_T}{\rho \mathrm{Pr}_T}\frac{\partial \overline{T}}{\partial z} \qquad 2.20$$

The Prandtl Number (Pr) in the energy equation represents the ratio of molecular diffusivity of momentum to the molecular diffusivity of heat. This ratio represents the relative growth of the velocity and thermal boundary layers. In this analysis the Prandtl number for the hot gas 0.55. This states that the thermal boundary layer outgrows the velocity boundary layer by a factor of 45%.

$$\mathrm{Pr} = \frac{\mu C_p}{k} = \frac{(0.00005673)(1006)}{0.10193} = 0.5599 \qquad 2.21$$

The Reynolds Averaged Navier Stokes (RANS) equations are time averaged equations that decompose the flow into mean and fluctuating components and produce the additional Reynolds Stresses. As shown, the k-epsilon model provides a way of computing the Reynolds Stresses and thus closing the system of equations. The Realizable k-epsilon model (RKE) is preferred over the Standard k-epsilon model (SKE) for boundary layer flows that contain separation and recirculation. The transport equations vary from standard k-epsilon model in the production of turbulent kinetic energy (k) and the transport of dissipation (ε). The main numerical difference is the C_μ term in the calculation of turbulent viscosity. The SKE model holds this term constant where the RKE model varies this value based on the strain of the flow.

For high strain flow, the RKE models have shown to be more accurate in transport and production of k and ε for turbo-machinery.

In the turbulence transport equations, G_k represents production of the kinetic energy from mean velocity gradients and G_b represents the production due to buoyancy. The Y_M term accounts for the effects of compressibility in the k-epsilon model.

$$\rho\frac{Dk}{Dt}=\frac{\partial}{\partial x}\left[\left(\mu+\frac{\mu_T}{\sigma_k}\right)\frac{\partial k}{\partial x}\right]+\frac{\partial}{\partial y}\left[\left(\mu+\frac{\mu_T}{\sigma_k}\right)\frac{\partial k}{\partial y}\right]+\frac{\partial}{\partial z}\left[\left(\mu+\frac{\mu_T}{\sigma_k}\right)\frac{\partial k}{\partial z}\right]+G_k+G_b-\rho\varepsilon-Y_M \quad 2.22$$

$$\rho\frac{D\varepsilon}{Dt}=\frac{\partial}{\partial x}\left[\left(\mu+\frac{\mu_T}{\sigma_\varepsilon}\right)\frac{\partial \varepsilon}{\partial x}\right]+\frac{\partial}{\partial y}\left[\left(\mu+\frac{\mu_T}{\sigma_\varepsilon}\right)\frac{\partial \varepsilon}{\partial y}\right]+\frac{\partial}{\partial z}\left[\left(\mu+\frac{\mu_T}{\sigma_\varepsilon}\right)\frac{\partial \varepsilon}{\partial z}\right]+\rho C_1 S\varepsilon-\rho C_2\frac{\varepsilon}{k+\sqrt{\nu\varepsilon}}+\frac{\varepsilon}{k}C_{\varepsilon 1}C_{\varepsilon 3}G_b \quad 2.23$$

$$G_k=\mu_T S^2 \quad 2.24$$

$$Y_M=\frac{\rho\varepsilon 2k}{a^2} \quad 2.25$$

$$C_1=\max\left[0.43,\frac{\eta}{\eta+5}\right] \quad 2.26$$

$$\eta=\frac{Sk}{\varepsilon} \quad 2.27$$

$$S=\sqrt{2S_{ij}S_{ij}} \quad 2.28$$

$$S_{ij}=\frac{\partial u'}{\partial x}+\frac{\partial v'}{\partial y}+\frac{\partial w'}{\partial z}+\left(\frac{\partial u'}{\partial y}+\frac{\partial v'}{\partial x}\right)+\left(\frac{\partial v'}{\partial z}+\frac{\partial w'}{\partial y}\right)+\left(\frac{\partial w'}{\partial x}+\frac{\partial u'}{\partial z}\right) \quad 2.29$$

The following constants have been formulated by curve fitting a wide range of turbulent flows as referenced by Tu et al [2].

$$\sigma_k=1.0\ ,\ \sigma_\varepsilon=1.3\ ,\ C_{\varepsilon 1}=1.44\ ,\ C_2=1.92$$

Due to steady state analysis the local acceleration terms are neglected. Additionally, since gravity is neglected the contribution of buoyancy (G_b) to the turbulence transport equations is also neglected.

$$G_b = \frac{\partial k}{\partial t} = \frac{\partial \varepsilon}{\partial t} = 0$$

2.2 Finite Volume Method

The Finite Volume Method (FVM) is the most widely applied method in CFD. The FVM is based on control volume integration and unlike Finite Differencing Schemes works well with structured and unstructured grids. The FVM utilizes the Gauss Divergence Theorem to evaluate cell centered values from values at the cell faces. The variable values at the cell faces are averaged values from the adjacent cell centers (First-Order Upwind) or the adjacent two cells (Second Order Upwind). Since the discrete equations are more diffuse than the original differential equations, the First Order Upwinding Method (FOU) introduces some numerical diffusion and even more where large gradients exist. However, the FOU method converges faster than SOU methods and can be used with higher Courant Numbers to increase convergence rates. The FOU scheme is utilized in this analysis since it is a design analysis and the convergence rate (or time) is a major factor in retrieving a design solution. For more information on the FVM method reference Tu, et al [2].

2.3 GAMBIT Software

GAMBIT (v2.2.30) Mesh Generation Software is a discretization software used to mesh the turbine blade model. The control volumes in this analysis represent the flow domain around the turbine blade and the solid blade. Discretization is the process of subdividing the volumes that represent the fluid and solid regions into smaller volumes called cells. In CFD, flow and thermal variables are solved from one of the cell to the next until the solution for the entire control volume is complete.

2.4 FLUENT Software

FLUENT (v6.3.26) is the commercial CFD software used to conduct aerodynamic and thermodynamic analysis in this report. FLUENT utilizes the discretized domain constructed in GAMBIT to solve the governing fluid and thermodynamic equations in throughout the control

volume. FLUENT does not contain an integrated meshing capability and must therefore be used in with GAMBIT or other mesh generation software.

2.5 Software Validation

Commercial CFD codes are commonly used in industry to assist in CFD analysis in an effort to reduce design cycle times and reduce the costs associated with experimental testing. Most end users, especially aerospace companies, are concerned with accuracy of such codes. Extensive efforts have been taken by CFD software companies to conduct validations of their codes. In this section validation of FLUENT is conducted on Turbine Blade Experiments published by the von Karmen Institute (VKI) of Technology [3] and NASA [7]. The experiments focus on aerodynamic properties such as velocity and thermodynamic properties such as heat transfer coefficient.

2.5.1 VKI Blade Validation

The first validation is conducted to compare the blade velocity distributions over a 2-dimensional turbine blade geometry. This is accomplished by comparing Schlieren Visualization results to blade pressure contours and by comparing Isentropic Mach Number distributions over the surface of the blade. This section covers three test points listed in table 2.1.

Table 2.1: VKI Blade Validation Test Points 1-3

	$T_{0,1}(K)$	$P_{0,1}(atm)$	M_{2IS}	$T_2(K)$	$P_2(atm)$	$\mu_1(\frac{kg}{ms})$	$L(mm)$	Tu_∞
Test 1	420	2.0	____	300	0	2.38e-5	3	1%
Test 2	420	0.647	0.875	300	0	2.77e-5	3	1%
Test 3	420	1.937	1.02	300	0	3.16e-5	3	1%

Evaluation of the pressure contours are compared to the Schlieren Visualization of the VKI experiment. Figure 2.1 shows is good visual correlation between experimental and FLUENT results. The shock formation on the suction side of the blade is characteristic of the actual blade experiment for transonic flow.

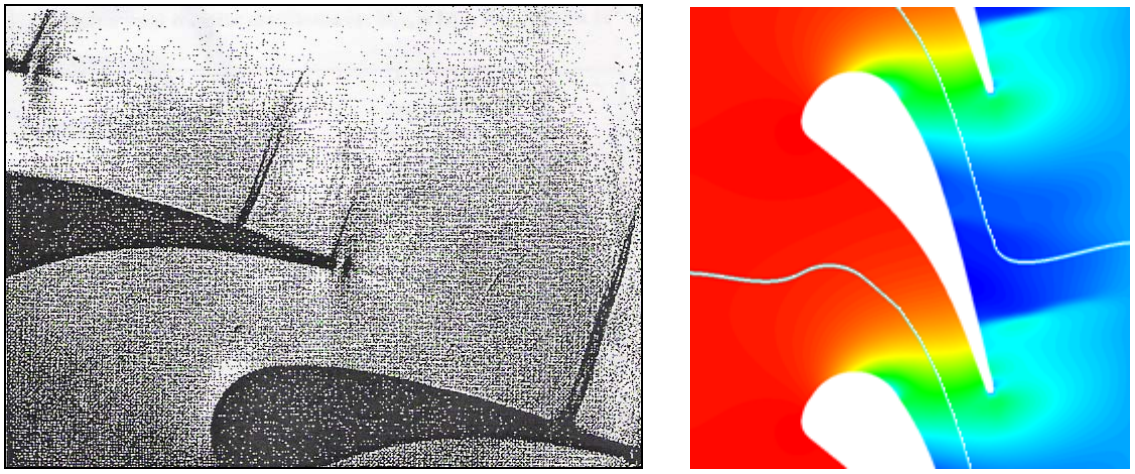

(a) (b)

Figure 2.1: Test 1 Pressure Contours (a) Schlieren Visualization [3] and (b) FLUENT Results

The blade velocity distributions are analyzed for two trailing edge Isentropic Mach Numbers of 0.875 and 1.02. The test parameters are listed as tests 2 and 3 of table 2.1. As shown in figure 2.2 for both test conditions, the FLUENT analysis shows comparable results to the experimental data. The Isentropic Mach numbers are computed using the isentropic pressure relation given in equation 2.30 and are plotted along the chord of the turbine blade in figure 2.2.

$$P_{01} = P_S\left(1+\frac{\gamma-1}{2}M_{IS}^2\right)^{\gamma/\gamma-1} \qquad 2.30$$

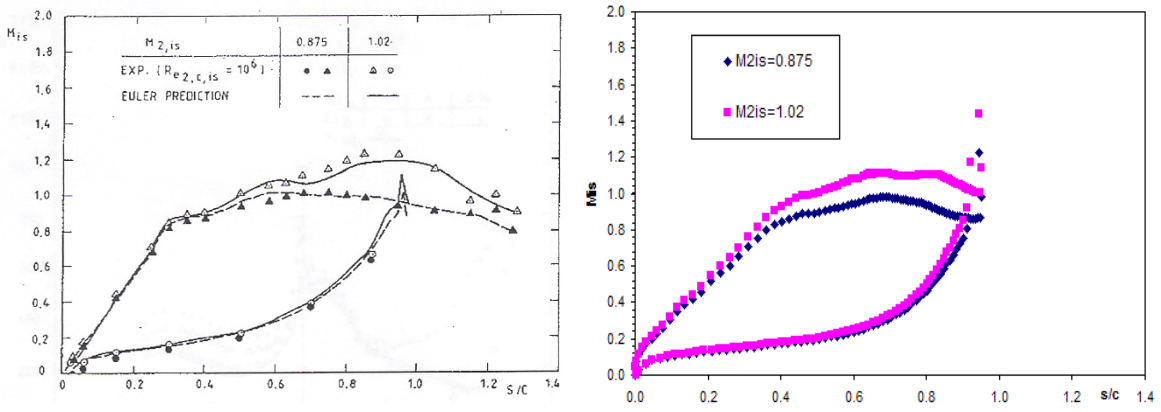

(a) (b)

Figure 2.2: Test 2/3 Isentropic Mach Number (a) VKI Results [3] and (b) FLUENT Results

2.5.2 NASA C3X Blade Validation

For validation of blade temperature distributions, a comparison was made to the NASA C3X blade. The data in this experiment was provided by NASA Lewis Research center by Hylton et al [7]. The thermodynamic data from the NASA C3X experiment is more conclusive than the VKI Blade and it analyzed internal cooling passages similar to that of this report. The test conditions compared in this analysis are listed in table 2.2. The test point for this comparison is referenced as code 5422 in the NASA report [7].

Table 2.2: NASA C3X Blade Validation Test Point 4

	$T_{0,1}(K)$	$P_{0,1}(Pa)$	Re_2	M_1	$T_2(K)$	$\mu_1(\frac{kg}{ms})$	$L(mm)$	Tu_∞
Test 4	796	107000	1.95E-6	0.17	300	3.707-5	16	8.3%

The static pressure distribution shows comparable results to experimental tests. Figure 2.3 compares experimental to FLUENT blade pressure distributions. The stagger in the FLUENT pressure distribution at 50% chord on the suction side is due to an error in the boundary layer mesh and is not an aerodynamic defect.

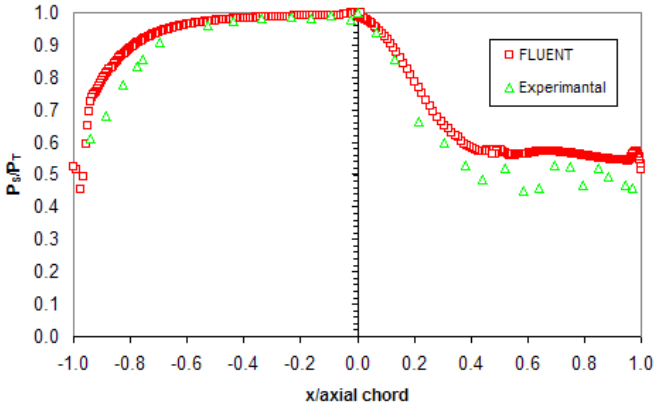

Figure 2.3: Test 4 Blade Pressure Distributions: NASA and FLUENT Results

The heat transfer coefficient for the same model is analyzed and compared. The heat transfer coefficient is computed from the heat flux and wall static temperature output from FLUENT. Using equation 2.31, the heat transfer coefficient is plotted versus blade chord in figure 2.4.

$$H_{tc} = \frac{\dot{q}_{face}}{(796K - T_{static,wall})} \qquad 2.31$$

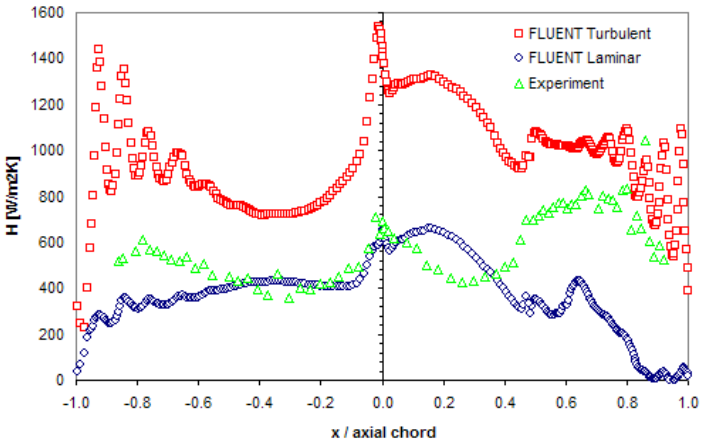

Figure 2.4: Test 4 Blade Heat Transfer Coefficient: NASA and FLUENT Results

From figure 2.4, it is seen that the heat transfer coefficient is over approximated in FLUENT near the leading edge when using a turbulence model. The current RKE model assumes turbulent flow over the entire blade. In the experimental analysis, the blade starts with laminar flow at the leading edge and transitions to turbulent flow at 20% chord. The current RKE model does not predict transition in the analysis. A simulation is run on the same configuration with laminar flow model. From Figure 2.4, the FLUENT laminar flow model accurately predicts the heat transfer coefficient near the leading edge. Additionally, the turbulent flow model appears to be more accurate near the trailing edge. A solution to this problem is to use a transition model or turbulent suppression across the turbine blade. Figure 2.5 shows the temperature distribution within the turbine blade and turbulence intensity around the blade as a result of the turbulent flow analysis.

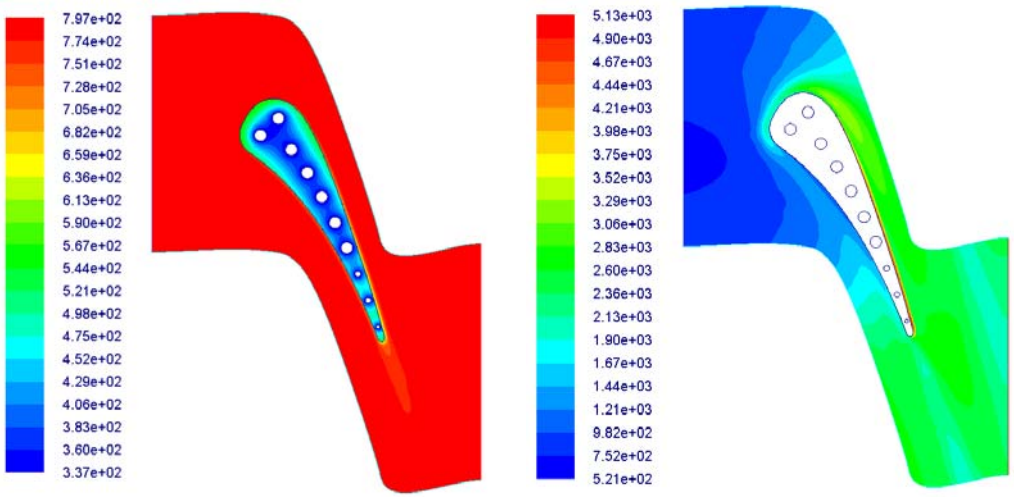

(a) (b)

Figure 2.5: NASA C3X Blade FLUENT Results
(a) Total Temperature (K) and (b) Turbulence Intensity

CHAPTER 3

OPTIMIZATION CODE

In this report, the optimization process is designed to reduce the maximum temperature within the blade structure to a value below a predefined maximum allowable temperature. In addition, the optimization aims to reduce the total integrated heat flux along the surface of the turbine blade. By reducing the total heat flux, the amount of cooling air required by the blade is also reduced. With these objectives, the final temperature in the blade will tend toward the maximum allowable. In addition to thermodynamic constraints, geometric constraints are also imposed on the blade design. These constraints can be related to structural or manufacturing requirements. A list of optimization constraints are listed in table 3.1.

Table 3.1: Thermodynamic Optimization Constraint

Parameter	**Dimension**
Maximum Temperature ($T_{\max}$)	1173.15 K

The initial blade design uses 30 individual cooling passages that are defined by radius (r_i) and position (x_i, y_i). The optimization code uses non-dimensional parameters to define cooling-passage positions normal (x_i) and tangent (y_i) to the outer surface of the blade. Table 3.2 lists the design limits of the turbine blade.

Table 3.2: Cooling Passage Design Constraints

Parameter	Lower Bound	Upper Bound
Radius (r_i)	0.5 mm	0.8 mm
Position (x_i)	1.0 mm	1.525 mm
Position (y_i)	$\frac{\bar{y}_{i-1} + \bar{y}_i}{2}$	$\frac{\bar{y}_i + \bar{y}_{i+1}}{2}$
Cooling Passage (i)	1	30
Minimum allowable distance between passages	1.0 mm	_____

The tangential cooling passage position (y_i) for the suction and pressure sides of the airfoil are constrained by equations 3.1 and 3.2, respectively. Where y_{te} is the y location of the trailing edge. This variable conversion is obtained from Dennis et al [1].

$$suction - side: \bar{y}_i = y_{te}(0.5451567 \tanh(\frac{\pi}{16}(i-1) - \frac{\pi}{2}) + 0.5) \quad 1 \le i \le 17 \qquad 3.1$$

$$pressure - side: \bar{y}_i = (1 - y_{te})(0.5451567 \tanh(\frac{\pi}{14}(i-17) - \frac{\pi}{2}) + 0.5) + y_{te} \quad 18 \le i \le 30 \qquad 3.2$$

The variable data from the optimization code is output to a file labeled “variables.txt”. The output lists three non-dimensional variable parameters per cooling passage resulting in 90 total variables. The convention for the non-dimension variables is listed in table 3.3. A copy of the variables for the initial design blade with 30 cooling passages is given in appendix [A]. Figure 3.1 depicts a 2D representation of the initial blade design.

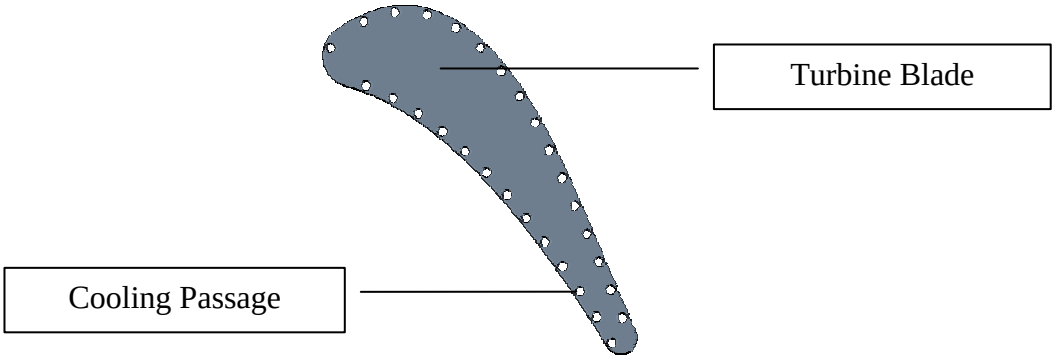

Figure 3.1: 2D Representation of Initial Design Turbine Blade

Table 3.3: Non-Dimensional Cooling Passage Variable Constraints

Description	**Variable**	**Constraint**
Number of Variables	90	constant
Hole Diameter	1.0000E-03	$0.001 < d_1 < 0.0016$
Hole Position Parallel to Edge	0.7167E-02	$0 < L_1 < 1$
Hole Position Perpendicular to Edge	0.1000E+00	$0 < n_1 < 1$

3.1 Overview of Genetic Algorithm Optimization

Genetic Algorithms (GA), in this analysis, optimize the performance of turbine blade cooling passage design. The algorithm evaluates design performance and subsequently compares and re-generates new designs. When a design is analyzed, fitness is assigned to the results. Fitness in this analysis is related to the thermodynamic performance of the turbine blade as analyzed by CFD software. Depending on the fitness of the result, the optimizer will apply selection, crossover and mutation operators to the design parameters. The design parameters include cooling passage radius (r) and position (x,y). These parameters are encoded using the base 2 binary system. Seven bit binary encoding is used for y and five bit binary encoding for x and r. In addition, the design parameters are grouped into a single binary string to represent a single geometric configuration. In the case of a turbine blade with 30 cooling passages the

structure is represented by (5*30)+(5*30)+(7*30)=510 bits. Figure 3.1.1 shows an example string used to define a blade configuration.

$$\underbrace{\underbrace{\underbrace{0110100}_{x_1}\underbrace{1010010}_{y_1}\underbrace{0100100}_{r_1}}_{hole_1}\underbrace{\underbrace{1111011}_{x_2}\underbrace{0100101}_{y_2}\underbrace{0101010}_{r_2}}_{hole_2}\underbrace{\underbrace{1101001}_{x_3}\underbrace{0100100}_{y_3}\underbrace{10010}_{r_3}}_{hole_3}}\ldots\ldots$$

Figure 3.2: Base 2 Binary String Encoding of Cooling Passage Variables

The optimization sequence is initiated using an even number of base designs. Each design is run through the analysis sequence to obtain a total integrated heat flux and maximum temperature. The performance of each design is evaluated and compared to the performance of the other designs. At this stage, the first GA operator of selection is applied by creating a tournament between the designs. The GA randomly matches up designs for a total of two matches per design. The designs winning each matchup get placed in the reproduction pool. Selection does not create new designs but simply duplicates the best performers at the expense of the worst performers. Figure 3.3 shows an example of natural selection where the lower number strings get duplicated, assuming lower numbers represent the best performers.

$$S1\_S2\_S3\_S4\_S5\_S6 \xrightarrow{selection} S1\_S1\_S2\_S2\_S3\_S4$$

Figure 3.3: Example of Natural Selection

The second GA operator of uniform crossover is applied to the reproduction pool. Two strings (called parents) are randomly selected from the reproduction pool. A uniform crossover of 50% is utilized in this analysis which means that 50% of the bits in a string are randomly chosen and exchanged between the two parents. This operation generates two new strings called children. This process is repeated until each parent has participated in the crossover operation. The crossover operation doubles the number of stings in the design pool. Once the children have been evaluated they will replace the parents in the design pool or they will be discarded based on performance.

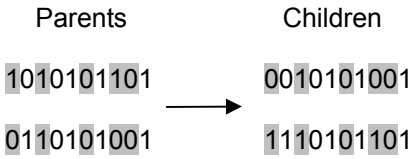

Figure 3.4: Example of 50% Uniform Crossover

The third GA operator is mutation. A 5% mutation operator is applied to all members (parents and children) in the design pool. The mutation operator selects a position in a design string and mutates it from 1 to 0 or vise versa. The 5% probability (p_m) effects the location of the bit to be mutated based on the selection of a random number $r \in [0,1]$. The next bit location is determined by equation 3.3. After the pool of designs has participated in reproduction, crossover and mutation, the designs area again evaluated for performance. The methods behind genetic algorithms can be referenced in Deb et al [6].

$$\eta = -p_m \ln(1-r) \qquad 3.3$$

Figure 3.4: Example of 5% Mutation

CHAPTER 4

TURBINE BLADE ANALYSIS

In conjunction with the GA optimization code, a sequence of analysis procedures is required to adequately model hot gas flow, convective heat transfer and heat conduction in and around a turbine blade. The objective is to adequately determine the integrated heat flux on the blade surface and the maximum temperature within the blade structure based on various cooling passage configurations. In addition to external flow analysis, a convective temperature distribution is specified along the span of cooling passages. Figure 4.1 displays a 2D representation of the blade discussed in this report. The representation depicts the primary hot gas path, the turbine blade and 30 cooling passages. Airfoil and boundary coordinates which will remain constant throughout the analysis can be found in appendix [A] labeled “airfoil points” and “boundary points”, respectively.

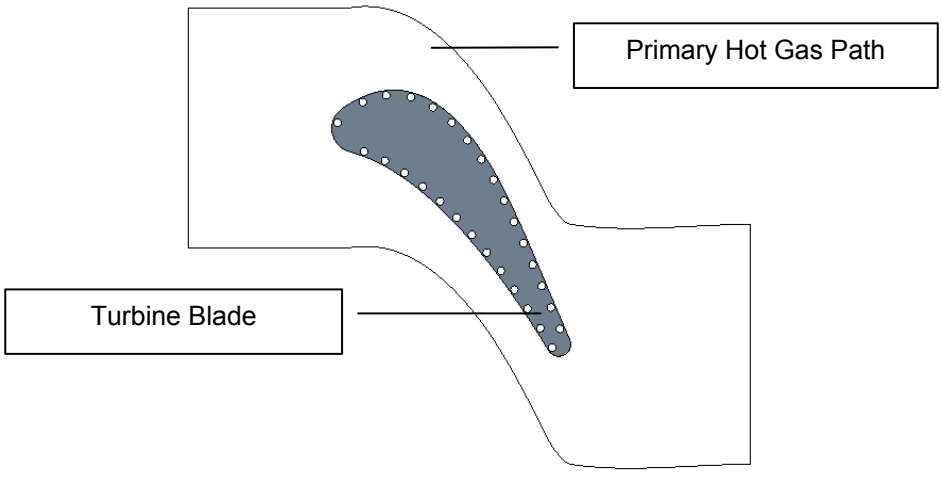

Figure 4.1: Airfoil Model with Primary Gas Path

Dimensions for the initial design of the cooling passages are listed in appendix [A] labeled “Hole Points”; however, size and location of the cooling passages will vary per design iteration.

Axial chord and span dimensions are given in table 4.1. The test conditions for the turbine blade analysis are listed in the boundary conditions section 4.4.2.

Table 4.1: Airfoil Shape Parameters

Parameter	Dimension
Axial Chord	5.0 cm
Span	5.0 cm

This section will outline the analysis procedure used to obtain the thermodynamic metrics used by the optimization code. As previously noted, a commercial CFD code (FLUENT) is used to conduct the fluid dynamic and thermodynamic analysis. The analysis process is setup to run automatically in order to evaluate multiple turbine blade designs as determined by the optimization code. For the analysis sequence to run automatically and autonomously, the process is setup to run in batch mode on a Linux parallel computing system. The details of the parallel system will be discussed in the parallel computing section 4.7. The analysis is designed to read cooling passage position variables from the optimization code and run a full aerodynamic and thermodynamic analysis on the turbine blade, focusing on the thermodynamic properties of the analysis. The flow chart in figure 4.2 depicts the sequence of procedures in the blade optimization and analysis. Procedures inside the black box are performed iteratively along with the optimization analysis and will be the focus of discussion in this chapter.

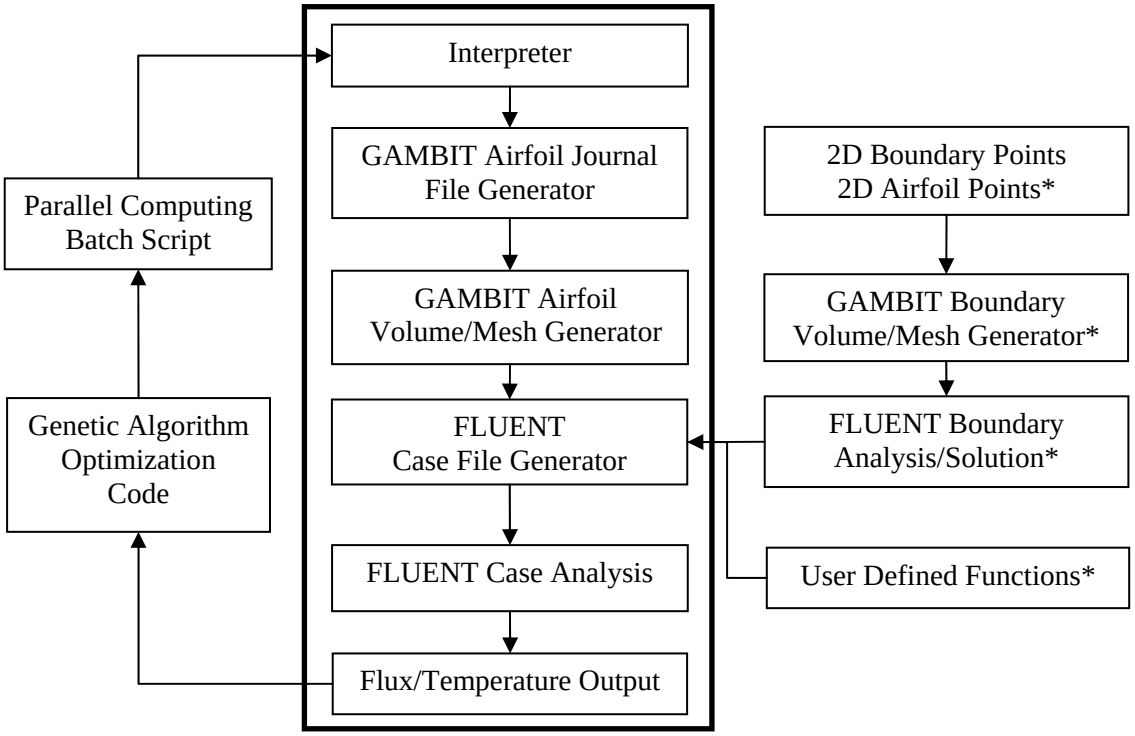

Figure 4.2: Procedure Flow Chart (*created once in the process)

4.1 Interpreter

The GA optimization code exports values of cooling passage location and diameter via a variable text file (vars.txt). The data defines the cooling passage location and diameter with three non-dimensional variables. The interpreter is a C code that converts non-dimensional cooling passage size and position data from the variable file into Cartesian coordinates and outputs the data to a file labeled holepoints.dat. Example files labeled “airfoil points” and “hole variables” can be found in Appendix A. Figure 4.3 depicts the data flow into and out of the interpreter.

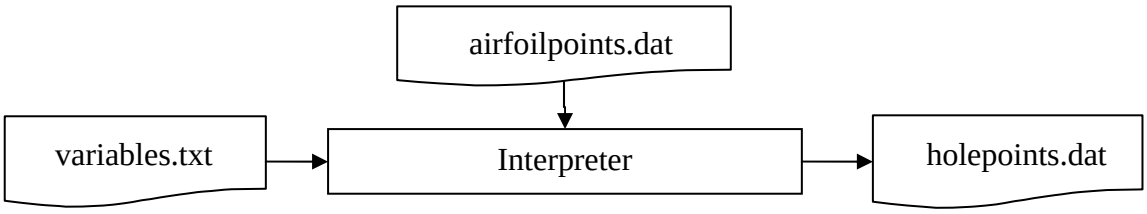

Figure 4.3: Interpreter Process Flow

4.2 GAMBIT Airfoil Journal File Generator

Once the 2-D cooling passage coordinates are generated they are combined with the airfoil to form a 3-D representation of the turbine blade. This procedure is accomplished using the GAMBIT mesh generation software. However, for GAMBIT to operate automatically, a journal file must be written to perform data import and mesh generation functions without use of the GUI. The journal file allows GAMBIT to run in batch mode on the parallel computing system. Since the blade geometry will change per iteration, the journal file must also change per iteration. A FORTRAN code is utilized to generate the GAMBIT journal file. The code utilizes two parameters from the "holepoints.dat" file discussed in section 4.1: 1) the number of cooling passages and 2) the number of data points per cooling hole. Therefore, the number of cooling passages can also change per design iteration and GAMBIT journal file will update accordingly. This procedure creates a journal file labeled "gambitjournal.jou" that is unique to the current turbine blade design. A copy of the Fortran code labeled "Journal File Generator" and an example journal file labeled "gambitjournal.jou" can be found in appendix A. These files are generated for and are applicable to only the initial blade design with 30 cooling passages and 19 data points per passage.

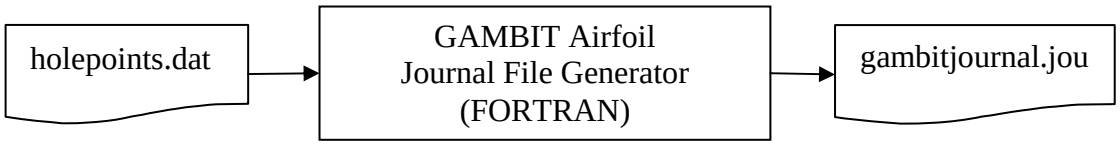

Figure 4.4: Journal File Generator Process Flow

4.3 GAMBIT Volume/Mesh Generator

With a current version of the GAMBIT journal file (gambitjournal.jou), a session of GAMBIT can be run automatically. Following predefined commands within the journal file, GAMBIT will import the 2D airfoil and cooling passage data points. The data points are used to create a 2D airfoil face with triangle mesh. The mesh parameters within the airfoil must be sufficient enough to resolve temperature gradients between the cooling holes and the surface of

the airfoil. This refinement is accomplished through the use of a boundary layer mesh around the perimeter of the cooling holes. By analyzing the worst case scenario with the largest cooling holes nearest the airfoil boundary, the mesh density can be made sufficient to capture the temperature gradients at the thinnest parts of the blade. During the geometry and mesh generation process, the number of mesh points on the boundary of the airfoil and cooling holes are defined. The surface mesh will triangulate itself based on the edge mesh and a maximum cell size specified. Figure 4.5 depicts the turbine blade mesh based on the parameters listed in table 4.2.

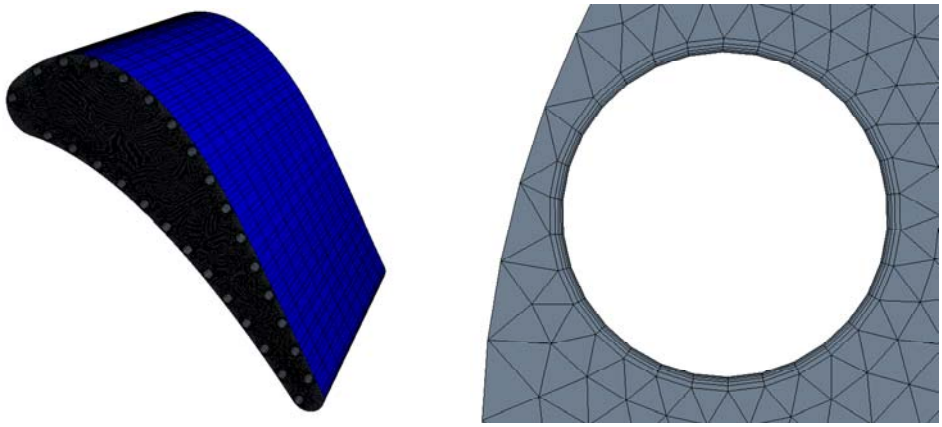

(a) (b)

Figure 4.5: Representation of (a) Airfoil Mesh and (b) Mesh around Cooling Passages

Table 4.2: Airfoil Mesh Parameters

Parameter	**Dimension**
Airfoil Perimeter Mesh Points	300
Cooling Hole Mesh Points	30
Cooling Hole Prism Layers	5
Prism Layer Growth Rate	1.5
1st Prism Layer Height	0.0005 cm

The resulting 2D mesh is a hybrid triangle and hexahedral mesh. The 3D representation of the airfoil is created by extruding the face with mesh by a factor -10. This generates an airfoil with 10 layers in the –z direction. Layering of the mesh serves two purposes: 1) to roughly capture the velocity and temperature gradients along the span of the blade and 2) to allow the application of convective temperature gradients along the cooling passages. The later will be discussed in Boundary Conditions section 4.4.3. Figure 4.6 shows the data process for this operation.

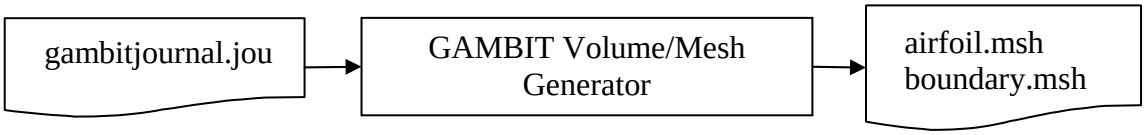

Figure 4.6: GAMBIT Volume/Mesh Generator Process Flow

Similarly, the boundary region (or primary gas path) of the airfoil is created and discretized. The airfoil and boundary domains are discretized separately to allow each region to be analyzed separately and later combined. With the optimized airfoil shape, the primary gas path is created using the curvature of the airfoil camber line and the blade pitch. Blade pitch is the distance between camber lines on adjacent airfoils. Pitch determines the distance of the top and bottom boundaries from the airfoil and is critical to blade performance since it inherently defines the distance between adjacent blades. Using periodic boundary conditions on the upper and lower boundaries, a single blade can be analyzed while capturing the cascade effect of adjacent blades.

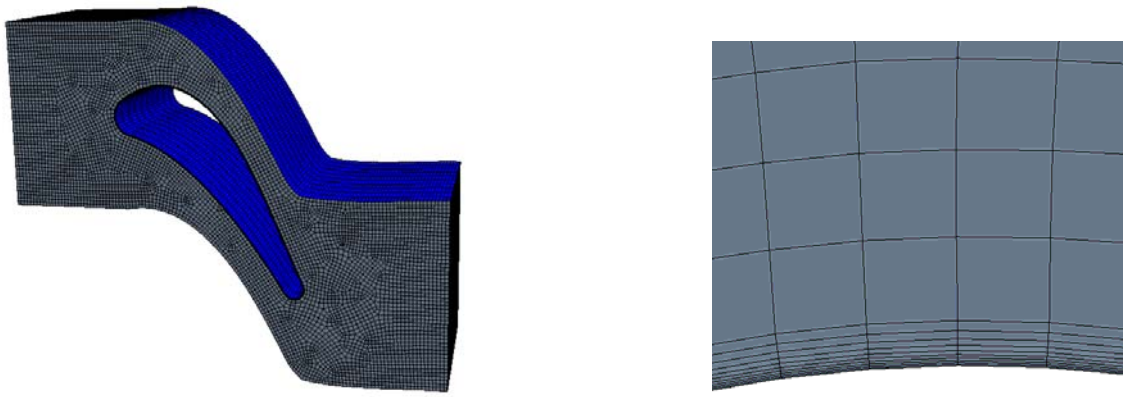

(a) (b)

Figure 4.7: Representation of (a) Boundary Mesh and (b) Boundary Layer Mesh

Figure 4.7 displays boundary mesh based on mesh parameters in table 4.3. Hexahedral based cells are used in the flow domain to achieve a structured discretization when possible. Additional, hexahedral based cells are less numerically diffusive since the cell faces are typically perpendicular and parallel to the flow.

Table 4.3: Boundary Mesh Parameters

Parameter	**Dimension**
Top/Bottom Edge Mesh Points	150
Inlet/Outlet Edge Mesh Points	50
Boundary Prism Layers	22
Dimensionless Wall Distance (y+)	1
Prism Layer Growth Rate	1.25
Near Wall Cell Height	0.00011 cm

One key component of the boundary mesh is the density and thickness of the boundary layer mesh. Resolution of the boundary layer near the wall is critical in obtaining the correct velocity profiles and temperature gradients along the airfoil. For accurate dimensioning of the boundary layer the dimensionless wall distance (y+) wall must be applied. The formulation of this value will be discussed in further detail in the Viscous Models section 4.4.4.

4.4 FLUENT Case File Generator

Before CFD analysis begins, a FLUENT case file is created to run the analysis. The case file is created in serial mode; therefore, the case file is generated and saved prior to running the analysis in parallel. The case file is in FLUENT file format and is created using a FLUENT journal file. The journal file lists FLUENT text commands that read mesh data, sets up boundary conditions, numerical solvers and writes the case file. A copy of the journal file labeled "fluent journal" is given in appendix A. The fluent journal file is interpreted by FLUENT and combines

As shown in figure 4.8, FLUENT interprets the journal file, combines the airfoil mesh, the boundary solution, User Defined Functions (UDF) and generates a FLUENT Case file. This process reduces the computation time for the airfoil solution by starting with a fully converged boundary solution.

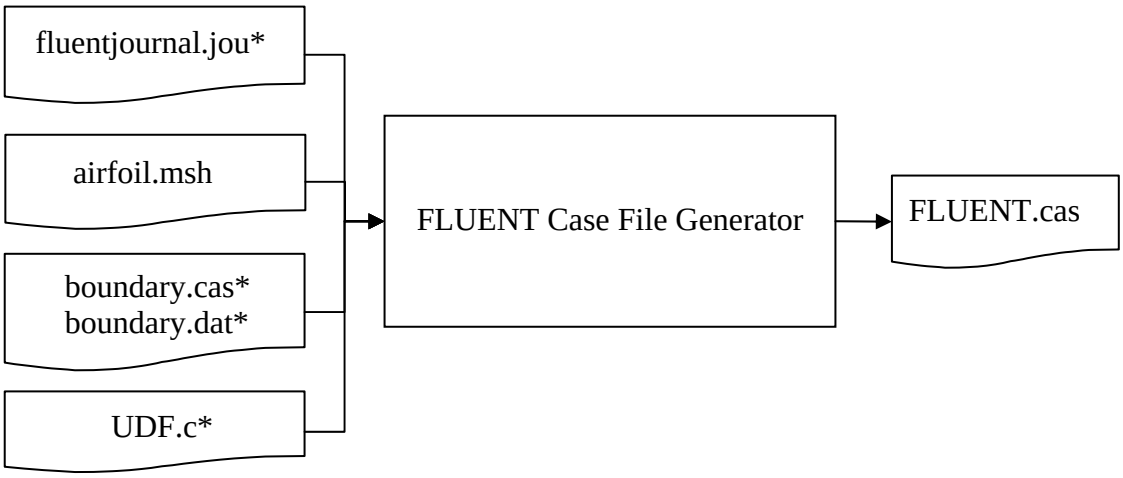

Figure 4.8: FLUENT Journal File Generator Process Flow

The boundary solution is computed prior to running the coupled boundary/blade solution. The reason for this is to reduce the computational time for the coupled solution. Since the airfoil geometry remains constant throughout the design process, the boundary solution is solved outside of the design loop and is coupled with each new blade design. The boundary solution is setup according to the parameters listed in table 4.2. The results of the boundary solution will be

discussed later in chapter 5. Figure 4.9 depicts the boundary solution without the turbine blade and the blade mesh. The remaining subsections describe the parameters used to setup the FLUENT case file for the parametric turbine blade analysis. Any value not explicitly given in this section will remain the FLUENT default value.

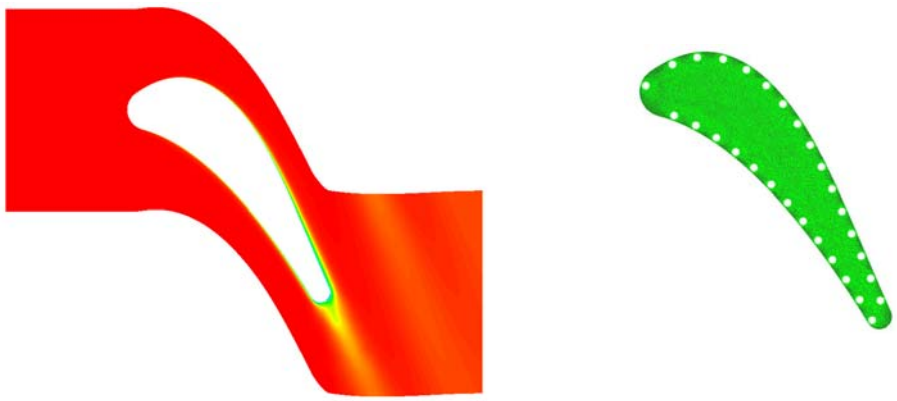

(a) (b)

Figure 4.9: Analysis Models (a) Boundary Solution and (b) Unsolved Blade Structure

4.4.1 Solvers

The solver used in FLUENT is the Coupled (or density based) Implicit solver. The coupled solver as the name implies is used for high speed compressible flow where there is a strong inter-dependence between density, energy and momentum. The coupled solver solves the continuity, momentum and energy equations simultaneously. The Implicit approach only deals with unsteady analysis and therefore has no significant bearing on the current steady analysis. Since energy is considered in this problem, the energy equation must be enabled for the current analysis. Viscous effects must also be considered in the numerical solver; therefore, the viscous k-epsilon model must be enabled with the Realizable option and standard wall functions. Wall functions will be discussed later in Viscous Models section 4.4.4.

4.4.2 Material Models

Materials used in the turbine blade analysis are Nickel (solid) and Air (fluid). The materials and material properties are selected from a material list embedded in FLUENT.

Density for fluid is set to ideal-gas since the fluid Mach Number exceeds 0.3. Refer to table 4.4 for material properties.

Table 4.4: Material Properties

Parameter	Hot Fluid (Air)	Solid (Nickel)	Cold Fluid (Air)
Density	$1.2\frac{kg}{m^3}(ideal-gas)$	$8900\frac{kg}{m^3}$	$1.2\frac{kg}{m^3}$ (constant)
Dynamic Viscosity	$5.673E-5\frac{kg}{m-s}$	——	$1.86E-5\frac{kg}{m-s}$
Specific Heat	$1006\frac{J}{kg-K}$	——	$460\frac{J}{kg-K}$
Thermal Conductivity	$0.10193\frac{W}{m-K}\Big\|_{T=1623K}$	$91.74\frac{W}{m-K}$	$0.0257\frac{W}{m-K}\Big\|_{T=298K}$

4.4.3 Boundary Conditions

Boundary conditions are a formal way of applying the test conditions to the geometric model. FLUENT supplies a suite of boundary types that can be applied to the model for various types of flow conditions. Since pressure differences across our blade are the main driving components of our flow we will use pressure inlet and outlet boundary conditions. As previously discussed, the top and bottom boundaries will be periodic translational boundaries since flow entering one boundary is identical to the flow exiting the other. At the interface of the boundary and the airfoil, the two boundaries are set as interface boundaries. This allows communication between the fluid mesh and the solid mesh. Table 4.5 lists the boundary types for all model boundaries. The test conditions applied to the boundaries are listed in table 4.2.

Table 4.5: Boundary Types and Conditions

Boundary	Boundary Type	Input Data
Inlet	Pressure Inlet	Total Gauge Pressure: 2 atm Total Temperature: 1623 K Static Gauge Pressure: 1 atm Turbulence Intensity: 1% Turbulence Viscosity Ratio: 100
Outlet	Pressure Outlet	Static Gauge Pressure: 0.0 atm
Boundary Top/Bottom	Translational - Periodic	_____
Boundary Front/Rear Airfoil Front/Rear	Symmetry	_____
Boundary Interface Airfoil Interface	Coupled - Interface	_____
Cooling Passages	Wall - Convection	Heat Transfer Coefficient: $994.96\frac{W}{m^2-K}$ Coolant Temp.: $298.15+57.9\sqrt{z/5}K$

Since the analysis neglects to analyze flow through the airfoil cooling passages, a calculation of the convective heat transfer coefficient in the cooling passages is made. This is accomplished by evaluating the Prandtl Number and Nusselt Number in the passages. An initial guess for the coolant mass flow is obtained from the NASA C3X blade example for a comparable diameter cooling passage. The resulting convective heat transfer coefficient listed in table 4.5 is computed from the following equations.

$$\Pr = \frac{C_p \mu}{k} \quad (4.1)$$

$$Nu = 0.23(\mathrm{Re}^{0.8})(\Pr^{0.4}) \quad (4.2)$$

$$HTC = \frac{kNu}{d} \quad (4.3)$$

4.4.3.1 User Defined Functions

The temperature variation along the span of the cooling passages is applied through a User Defined Function (UDF) in FLUENT as a convective boundary condition. The UDF is a C code of the coolant temperature variation listed in table 4.5. The cooling passage exit temperature and the temperature variation along the span of the cooling passages is approximated by Dennis et al [1] by the following equations.

$$T_{exit} = T_{wall} - (T_{wall} - T_{inlet})e^{-\frac{h_c \pi d L}{\dot{m} C_p}} \quad (4.4)$$

$$T_{coolant} = T_{inlet} - (T_{inlet} - T_{exit})\sqrt{\frac{z}{L}} \quad (4.5)$$

The UDF reads position data from each cell face along the cooling passage and assign the cell face with an ambient temperature that varies along the span of the cooling passage. This temperature variation simulates the rise in temperature that the cooling fluid experiences as it absorbs heat from the blade structure. This ambient temperature reference (z-temperature) is used in the convection wall boundary condition of the cooling passages. A copy of the C code labeled “User Defined Function” can be found in appendix A.

4.4.4 Viscous Models

Viscous models are used to accurately predict the turbulent behavior of the fluid flow. For this analysis the Realizable k-Epsilon turbulence model is selected. The k-epsilon model is primarily formulated for confined flows such as that experienced in turbine blade cascades and for high Reynold’s Number flows. The governing equations for the k-epsilon model were previously formulated in section 2.1.4.

Since transport equations only compute cell centered values, a methodology must be employed to link the cell values to values at the wall. Wall functions are used to bridge the gap between the wall and the computation cells near the wall. Wall functions are semi-empirical formulas and functions that link (or bridge) the solution at the near wall cells to the corresponding quantities on the wall. Wall functions are comprised of law-of-the-wall formulation for mean velocity and temperature and formulas for near wall turbulent quantities. The process for applying wall functions to wall bounded flows depends on the grid resolution near the wall. There are two primary grid resolution categories under which wall functions are employed: 1) high y+ and 2) low y+.

To determine the appropriate grid resolution near the airfoil, we must first understand turbulent flow behavior. Figure 4.10 depicts the flow behavior over a flat plate. As shown, the turbulent flow region is comprised of three layers. The first layer is the viscous sub layer where viscous effects are dominant. The second layer is the buffer zone between the viscous sub-layer and the turbulent layer. The third layer is the turbulent (or log-law) layer where the turbulent effects are dominant. The turbulent layer is bounded by the free stream flow and depends on Reynolds Number.

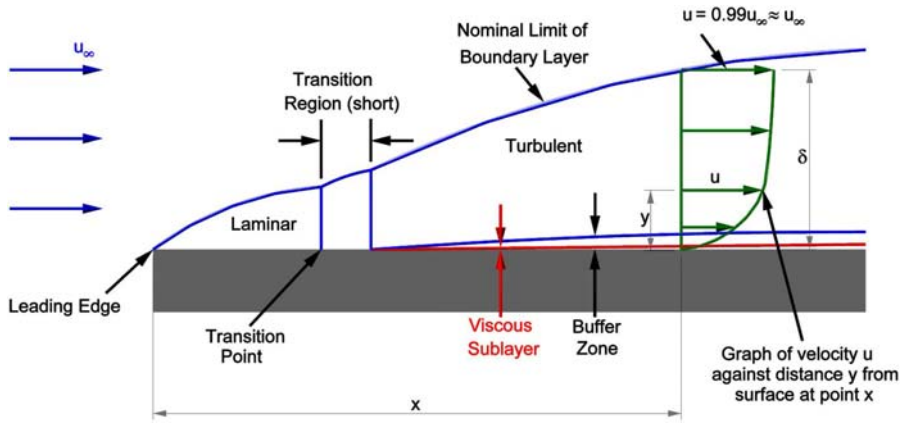

Figure 4.10: Flat Plate Laminar to Turbulent Transition

Figure 4.11 gives a representation of each layer and their respective y+ location from the wall. The y+ value is a non-dimensional distance from the wall to the first near wall cell. As shown, the viscous sub-layer extends from $0 \le y+ \le 5$ and the turbulent layer $60 \le y+ \le 200$.

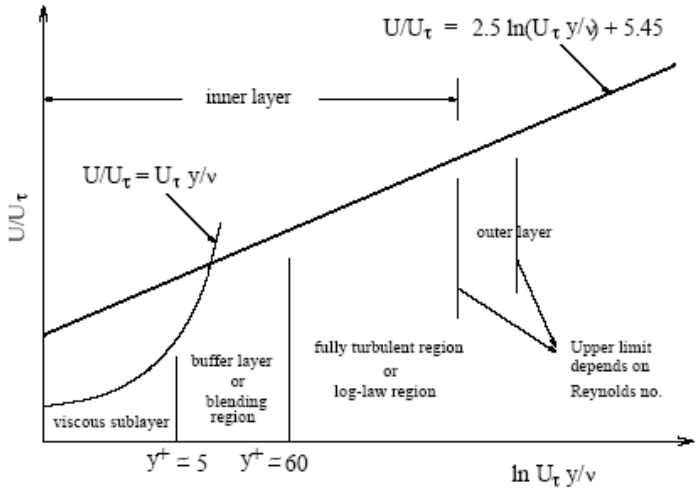

Figure 4.11: Turbulent Boundary Layer Regions

For high Reynolds number flows such as this analysis, the theoretical y+ value of the near wall cell will be in a range of 60 to 200. However, since we are evaluating conjugate heat transfer the y+ is set for low Reynolds flows at a value of 1. This reduces the height of the near wall cells and increases the number of prism layers required to resolve the turbulent boundary layer. Values for near wall cell height, growth rate and number of prism layers are listed in table 4.3. The equations used to compute the near wall cell height are derived from Wall Function Theory. The actual near wall cell height (y) is approximated using equations 4.6, 4.7 and 4.8. Here U is the local velocity based on the flow Reynolds Number, $u+$ is the non-dimensional local velocity and U_τ is defined as the friction velocity at the nearest wall. Implementing values for local velocity, kinematic viscosity and y+ will result in a value for the near wall cell location(y).

$$y+ = \frac{U_\tau y}{\nu} \qquad 4.6$$

$$u+ = \frac{U}{U_\tau} \tag{4.7}$$

$$u+ = 2.5\ln(y+) + 5.45 \tag{4.8}$$

During computation, for y+ values less than 11.225, FLUENT uses a linear stress-strain relationship between y+ and u+. This means that the log law is ignored and the velocity between the wall and the near wall cell is computed straight from the wall shear stress.

$$U = U_\tau^2 \frac{y}{\nu} \tag{4.9}$$

$$U_\tau = \sqrt{\frac{\tau_w}{\rho}} = \sqrt{\frac{\mu}{\rho}\left(\frac{\partial u}{\partial y}\right)_{y=0}} \tag{4.10}$$

Similarly, the temperature is also approximated using wall functions. In the temperature solution, the non-dimensional thermal sub layer thickness (y_T+) is defined as the intersection between the logarithmic and linear thermal laws. These laws are defined as follows.

$$\frac{(T_W - T)\rho C_p C_\mu^{1/4} k^{1/2}}{\dot{q}} = \begin{cases} \left[\Pr(y+) + \dfrac{\rho \Pr C_\mu^{1/4} k^{1/2} U^2}{2\dot{q}}\right]_{y+<y_T+} \\ \left[\Pr_T\left[2.38\ln(9.793y+) + P\right] + \dfrac{\rho C_\mu^{1/4} k^{1/2}}{2\dot{q}}\left[\Pr_T U^2 + (\Pr - \Pr_T)U_C^2\right]\right]_{y+>y_T+} \end{cases} \tag{4.11}$$

$$P = 9.24\left[\left(\frac{\Pr}{\Pr_T}\right)^{3/4} - 1\right]\left[1 + 0.28e^{-.007\,\Pr/\Pr_T}\right] \tag{4.12}$$

Depending on the relationship between the near wall cell y+ value and the thermal sub-layer thickness (y_T+), a linear or logarithmic equation is used to compute either the wall temperature (T_W) or the heat flux (q).

Due to the resolution of the grid near the airfoil surface, the solver is able to resolve the flow down to the viscous sub-layer; therefore, standard wall functions can be selected in the solver for near wall conditions.

4.4.5 Solution Controls

Solution controls are used to control the direction of the solvers in the FLUENT numerical analysis. Under-Relaxation Factors, Courant Number and Discretization Schemes can be modified in FLUENT to provide faster convergence or control stability of a solution. The following sections will give a description of each control factor in FLUENT.

4.4.5.1 Under-Relaxation Factors

Under-Relaxation Factors are used by the solver to control or limit the amount of influence the previous iteration has over the present iteration. When using the coupled solver, only the non-coupled turbulence equations utilize under-relaxation. FLUENT provides default under-relaxation factors that work well in most situations. The following equations depicts the relationship between the under-relaxation factor (α) and the scalar value (ϕ) and the computed change in scalar value ($\Delta\phi$).Table 4.6 lists the default under-relaxation factors used in this analysis.

$$\phi_{new} = \phi_{old} + \alpha\Delta\phi \qquad 4.13$$

Table 4.6: FLUENT Under-Relaxation Factors

Parameter	Dimension
Turbulent Kinetic Energy	0.8
Turbulent Dissipation Rate	0.8
Turbulent Viscosity	1.0
Solid	1.0

4.4.5.2 Courant Number

The coupled set of governing equations is discretized in time for both steady and unsteady calculations. However, in a steady state analysis the time marching proceeds until a steady state solution is reached. For steady analysis the Courant Number can be thought of as a representing a relaxation factor. Here the Courant Number (CN) is defined in equation 4.8 and

is represented by the largest velocity component in a given cell (u), time step (Δt) and cell size (Δx) in the direction of velocity. When advection dominates diffusion, a CN value less than unity will decrease oscillations in the residuals, improve accuracy and decrease numerical diffusion.

$$CN = u\frac{\Delta t}{\Delta x} \qquad 4.14$$

For the blade analysis, the Courant Number is initially set low to maintain stability then increased to increase analysis convergence. Table 4.7 lists the courant numbers and corresponding iterations for the blade analysis.

Table 4.7: Courant Number vs. Iteration

Iteration	**Courant Number**
1-200	2
201-400	5
401-1000	7

4.4.5.3 Discretization Scheme

As previously noted for the flow, a First Order Upwind Scheme is utilized to evaluate the fluid flow variables. In addition, the first order upwinding scheme is used to evaluate turbulent quantities of kinetic energy and dissipation. First Order Upwinding, as applied to the finite volume method, means that the scalar quantities at the cell faces of the current cell are derived from the upstream cell values. Upwinding is a method of weighting the upstream values to influence the current cell face values. Second Order Upwinding utilizes the cell face value at the two adjacent cells to derive the face values at the current cell.

Table 4.8: Discretization Schemes

Parameter	Scheme
Flow	First Order Upwind
Turbulent Kinetic Energy	
Turbulent Dissipation Rate	

4.5 FLUENT Analysis

Once the FLUENT case file is generated, analysis is run on the current turbine blade design. The case file from the previous step is reopened in a parallel version of FLUENT. Control of FLUENT is accomplished through the use of an input file labeled “Parallel Input” which can be found in appendix A. The parallel input file reads the existing FLUENT case file, initializes the solution, assigns the Courant Number, assigns the number of iterations and runs the FLUENT until the maximum number of iterations have been meet. The number of iterations depends on the convergence of the solution in the boundary and turbine blade. Details of the parallel computing system are discussed in the following section.

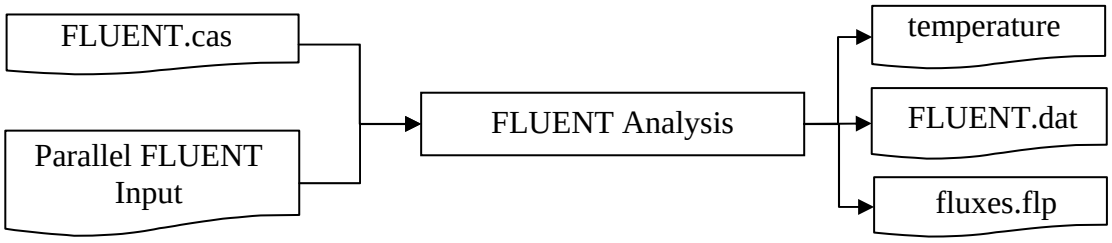

Figure 4.12: FLUENT Analysis Process Flow

The resulting analysis runs 1000 iterations of FLUENT to obtain a converged boundary and blade solution. Convergence is based on numerical residuals and the convergence of the integrated heat flux on the surface of the turbine blade. The analysis results in the creation of a FLUENT data (.dat) file, a temperature file (temperature) that lists the temperature at each computational node within the blade structure and a flux file (.flp) that lists the total integrated

heat flux on the blade surface. These values are used by the optimizer to evaluate design performance. Blade design results are discussed in chapter 5.

4.6 Parallel Computing System

The computing resources used to run the CFD analysis where provided by the University of Texas at Arlington CFD lab. The parallel cluster is a Linux based operating system with 9 nodes and 2 processors per node. Each processor is a 2.8 GHz processor with 2GB of RAM. The design iterations are setup to run on three nodes. For each analysis, one processor acts as the head node and distributes and collects data from the remaining 5 processors. The remaining 5 do the computational work of the analysis. Since the performance of the analysis does not scale linearly with the number of nodes, utilizing more nodes will only fractionally reduce the compute time for each analysis. Additionally, using three nodes per analysis allows three different analyses to run simultaneously on the system. Each step in the analysis process from the interpreter to the output file generator is scripted to run in “batch mode” on the parallel system. Batch mode allows the process to be run without human interaction. The batch script lists all the commands required to run the analysis and essentially links all the input, individual codes and output together. The batch script is also used to dictate the name of the jobs and the number of nodes to run. A copy of the batch script is provided in appendix A labeled “Batch Script”.

CHAPTER 5

TURBINE BLADE ANALYSIS RESULTS

This chapter will cover the results of various turbine blade designs. The designs presented are a formulation of work required to setup the design process outlined in chapter 4 and the results of the design iterations. The results presented will outline the analysis of an un-cooled turbine blade, the initial design turbine blade and the final design turbine blade.

5.1 Base Turbine Blade Design (Un-Cooled)

Analysis of an un-cooled turbine blade gives us, as Engineers, a representation of the aerodynamic and thermodynamic conditions that turbine blade work under. In addition, the un-cooled analysis serves as a reference point to the performance of the cooled blades latter discussed. The un-cooled turbine blade is subject to the same test conditions as the cooled blades. In addition, analysis of the un-cooled blade will provide an opportunity see the aerodynamics of the blade without cooling.

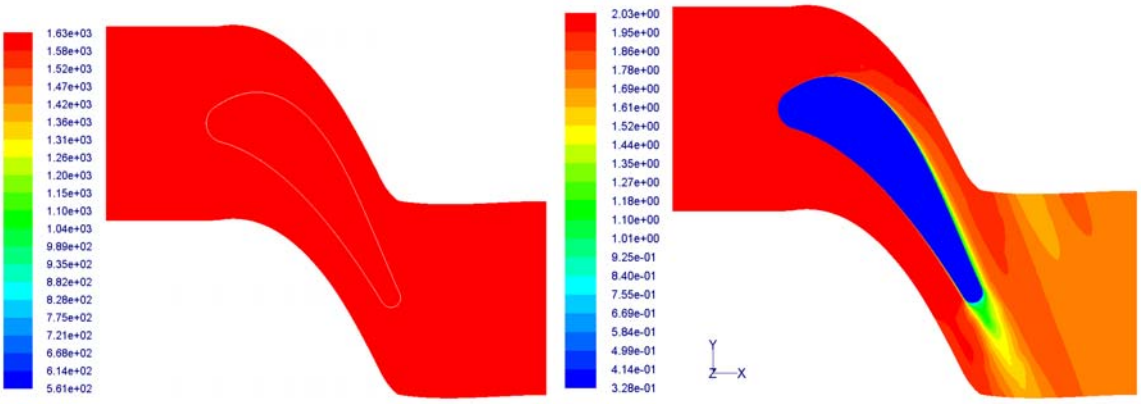

(a) (b)

Figure 5.1: Base Turbine Blade Design (Un-Cooled)
(a) Total Temperature (K) and (b) Total Pressure (atm)

Figure 5.1 displays the total temperature and total pressure profiles in the blade. The range on the total temperature scale in set at the same range for the cooled blade for comparison. Actual losses in total temperature can be seen in figure 5.2 (a). For the un-cooled turbine blade, the total surface heat flux and maximum temperature are listed in table 5.1. Once the blade has reached its maximum thermal capacity, the heat flux from the hot gas will reduce to zero at which time the maximum temperature within the blade is reached. Maximum temperature within the blade is experienced at the leading edge due to its proximity to the incoming flow and the lack of thermal boundary layer.

Table 5.1: Thermal Properties for Base Turbine Blade Design (Un-Cooled)

Parameter	Dimension
Total Surface Heat Flux	0.0 W
Maximum Temperature in Airfoil	1613 K

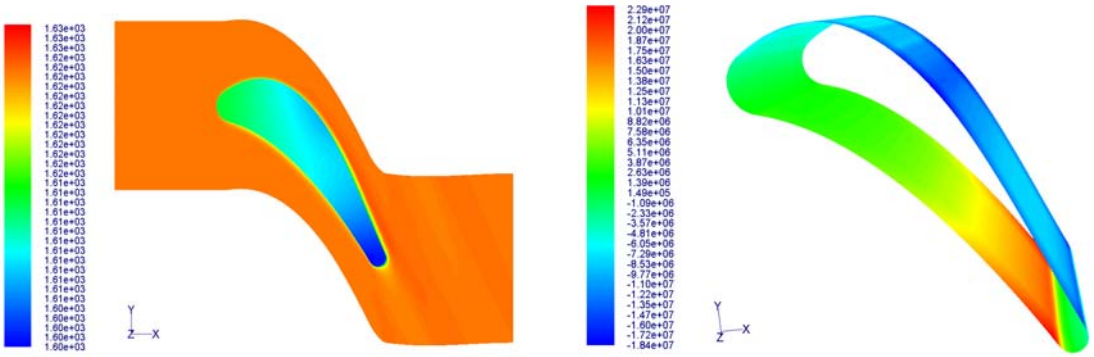

(a) (b)

Figure 5.2: Base Turbine Blade Design (Un-Cooled)
(a) Total Temperature (K) and (b) Vorticity (/s)

Figure 5.2 (a) shows the actual variation of total temperature in the blade structure. Figure 5.2 (b) shows vorticity contours at the airfoil surface. Vorticity increases the amount of heat transfer from the blade surface to the hot gas; however, due to the reduction of temperature at the trailing edge due to the thermal boundary layer, the trailing edge does not reach the same temperatures as the leading edge.

5.2 Initial Turbine Blade Design (Cooled)

The objective of this report is to create a turbine blade with internal cooling passages. The initial design case used to setup the analysis is presented here. This case uses 30 internal cooling passages to cool the blade by convective heat transfer from the cool air within the cooling passages to the blade structure. Figure 5.2 shows temperature contours of the cooling passages and the temperature gradient along the z-axis. The temperature gradients represent the heating of the cool air from the blade structure.

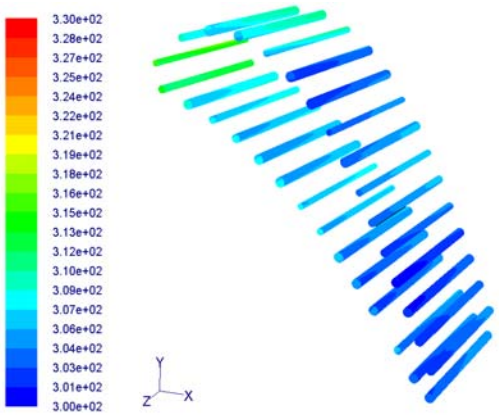

Figure 5.3: Initial Turbine Blade Design Cooling Passage Temperature (K)

As illustrated in figure 5.4, cooling passages reduce the maximum temperature within the blade structure and increases the heat flux across the blade surface. Here, the blade experiences a characteristic loss in total temperature and total pressure.

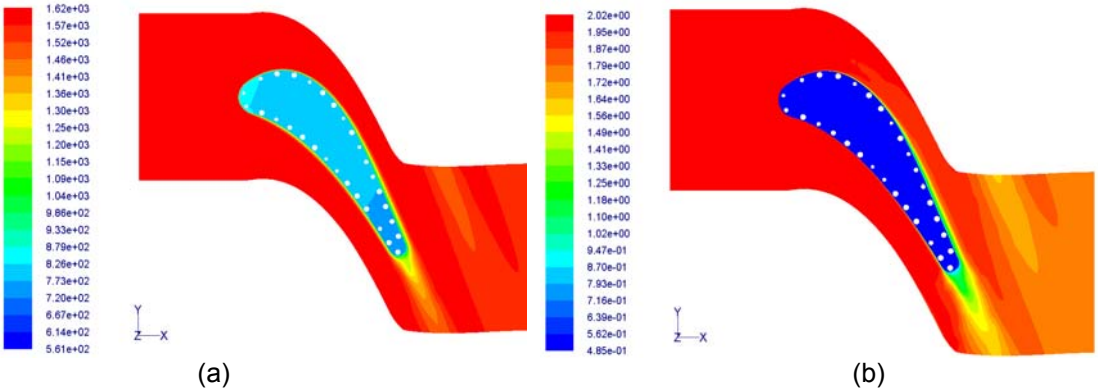

(a) (b)

Figure 5.4: Initial Turbine Blade Design (Cooled)
(a) Total Temperature (K) and (b) Total Pressure (atm)

Table 5.2: Thermal Properties for Initial Turbine Blade Design (Cooled)

Parameter	Dimension
Total Surface Heat Flux	1573 W
Maximum Temperature in Airfoil	340 K

Following the same test conditions as the un-cooled blade an analysis of the cooled blade is conducted.

5.3 Improved Turbine Blade Design (Cooled)

After running 10 iterations of the GA Optimization Code the solution is an improved design over the un-cooled and initial design blades in sections 5.1 and 5.2, respectively. The improved design blade shows a clustering of cooling passages near the leading edge of the airfoil to combat the maximum static temperature experienced in the initial design blade. The objective of the optimization code was to increase the temperature inside the blade up to a maximum total temperature of 1173.15 K. The improved turbine blade increases to a static temperature of 885 K and inherently reduces the total heat flux across the blade surface to 1459 W as listed in table 5.3. The resulting cooling passage variables can be found in Appendix A labeled “Improved Hole Variables”.

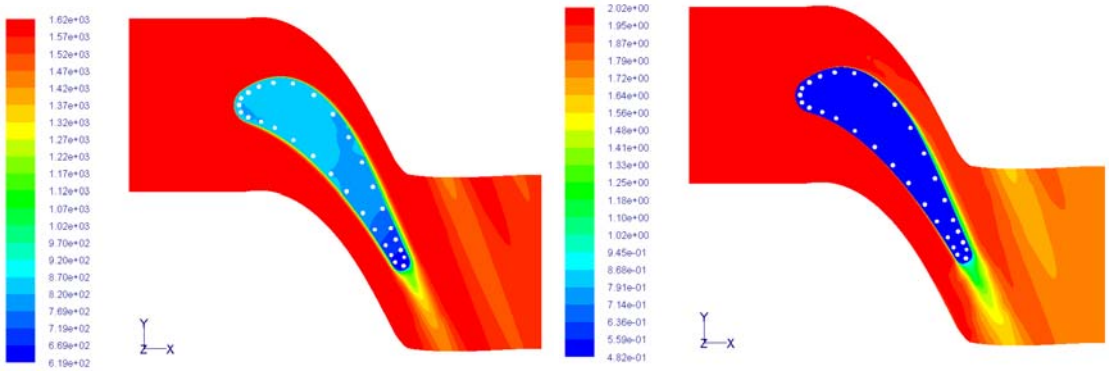

(a) (b)

Figure 5.5: Improved Turbine Blade Design (Cooled)
(a) Total Temperature (K) and (b) Total Pressure (atm)

Table 5.3: Thermal Properties for Improved Turbine Blade Design (Cooled)

Parameter	Dimension
Total Surface Heat Flux	1459 W
Maximum Temperature in Airfoil	855 K

5.4 Future Work

There are several suggestions that can be made from the experience gained in this analysis. Several different view points can be taken in this analysis from the perspective of discretization, numerical methods, parallel computing methods and model setup. Some decisions where made in the setup of this analysis that sacrifice accuracy for speed and vice versa. Some suggestions are subsequently discussed.

First, first order upwinding schemes are used in the flow analysis. This decision was made to increase speed in the computational analysis. Second order upwinding schemes provide more accurate results at the expense of increased computational time. An analysis will need to be done to compare the variation in the solution and computational time from one method to another.

Second, the blade was modeled with symmetry planes at the front and rear (not inlet and outlet) of the boundary and airfoil. This was done to reduce the wall effects on the hot gas flow. This decision produced symmetric results on the blade analysis; however, this resulted in a more computationally intensive analysis. Changing one or both sides of the airfoil/boundary to walls will greatly reduce the computational time and more accurately model blade turbine blade hubs and shrouds

Third, the turbulence models used in this analysis do not predict laminar to turbulent transition. They essentially assume turbulent flow on all parts of the blades. As seen in the validation section of this report, this greatly affects the heat flux from the free-stream to the airfoil. This turbulence assumption increases the turbulence intensity near the leading edge of

the airfoil and effects heat transfer in this region. It is suggested to research the ability to model transition in FLUENT or to suppress the onset of transition on the blade surface.

Fourth, if the number of cooling holes and the number of data points per cooling hole remain constant, then a single GAMBIT journal file can be used to generate the volume and mesh for all design iterations. This eliminates the need for the FORTRAN GAMBIT File Generator.

Fifth, the amount of cells used to discretize the airfoil domain is significantly greater than that required to solve the similar C3X blade temperature profile. Decreasing the amount of cells interior to the blade will inherently reduce the computation time on the structure. This procedure is required to be changed in the discretization phase of the process.

APPENDIX A

SUPPORTING DOCUMENTS

Hole Variables

90
1.0000000E-03
0.7166667E-02
0.1000000E+00
1.2000000E-03
5.0000000E-02
0.0000000E+00
1.6000000E-03
8.3333333E-02
0.0000000E+00
1.6000000E-03
1.1666667E-01
0.0000000E+00
1.1000000E-03
1.5000000E-01
0.0000000E+00
1.6000000E-03
1.8333333E-01
0.0000000E+00
1.6000000E-03
2.1666667E-01
0.0000000E+00
1.0000000E-03
2.5000000E-01
0.0000000E+00
1.6000000E-03
2.8333333E-01
0.0000000E+00
1.1000000E-03
3.1666667E-01
0.0000000E+00
1.3000000E-03
3.5000000E-01
0.0000000E+00
1.3000000E-03
3.8333333E-01
0.0000000E+00
1.6000000E-03
4.1666667E-01
0.0000000E+00
1.6000000E-03
4.5000000E-01
0.0000000E+00
1.5000000E-03
4.8333333E-01
0.0000000E+00
.....

.....
1.6000000E-03
5.1666667E-01
0.0000000E+00
1.6000000E-03
5.4500000E-01
0.0000000E+00
1.6000000E-03
5.6633333E-01
0.0000000E+00
1.3000000E-03
6.0066667E-01
0.0000000E+00
1.6000000E-03
6.5000000E-01
0.0000000E+00
1.6000000E-03
6.8333333E-01
0.0000000E+00
1.6000000E-03
7.1666667E-01
0.0000000E+00
1.1000000E-03
7.5000000E-01
0.0000000E+00
1.0000000E-03
7.8333333E-01
0.0000000E+00
1.6000000E-03
8.1666667E-01
0.0000000E+00
1.6000000E-03
8.5000000E-01
0.0000000E+00
1.4000000E-03
8.8333333E-01
0.0000000E+00
1.2000000E-03
9.1666667E-01
0.0000000E+00
1.6000000E-03
9.5000000E-01
0.0000000E+00
1.2000000E-03
9.8233333E-01
0.0000000E+00

Airfoil Points

x	y	z	x	y	z	x	y	z	x	y	z
0.0000	9.0000	0.0000	5.7744	8.7087	0.0000	9.8335	0.4848	0.0000	6.3906	3.6208	0.0000
0.0011	9.0230	0.0000	5.8545	8.6086	0.0000	9.8461	0.4564	0.0000	6.3068	3.7254	0.0000
0.0020	9.0460	0.0000	5.9335	8.5072	0.0000	9.8583	0.4287	0.0000	6.2220	3.8298	0.0000
0.0031	9.0690	0.0000	6.0115	8.4045	0.0000	9.8703	0.4017	0.0000	6.1364	3.9343	0.0000
0.0045	9.0922	0.0000	6.0885	8.3007	0.0000	9.8819	0.3753	0.0000	6.0500	4.0386	0.0000
0.0066	9.1155	0.0000	6.1644	8.1958	0.0000	9.8932	0.3496	0.0000	5.9627	4.1428	0.0000
0.0095	9.1390	0.0000	6.2392	8.0897	0.0000	9.9042	0.3244	0.0000	5.8747	4.2466	0.0000
0.0131	9.1626	0.0000	6.3129	7.9827	0.0000	9.9150	0.2998	0.0000	5.7859	4.3502	0.0000
0.0174	9.1864	0.0000	6.3853	7.8747	0.0000	9.9256	0.2756	0.0000	5.6964	4.4533	0.0000
0.0224	9.2105	0.0000	6.4564	7.7657	0.0000	9.9358	0.2519	0.0000	5.6061	4.5560	0.0000
0.0280	9.2348	0.0000	6.5263	7.6559	0.0000	9.9459	0.2286	0.0000	5.5152	4.6581	0.0000
0.0343	9.2594	0.0000	6.5948	7.5452	0.0000	9.9558	0.2057	0.0000	5.4237	4.7596	0.0000
0.0413	9.2842	0.0000	6.6620	7.4338	0.0000	9.9653	0.1831	0.0000	5.3316	4.8604	0.0000
0.0491	9.3094	0.0000	6.7278	7.3218	0.0000	9.9736	0.1604	0.0000	5.2389	4.9605	0.0000
0.0577	9.3349	0.0000	6.7926	7.2092	0.0000	9.9807	0.1376	0.0000	5.1457	5.0598	0.0000
0.0673	9.3607	0.0000	6.8563	7.0962	0.0000	9.9867	0.1147	0.0000	5.0520	5.1581	0.0000
0.0778	9.3868	0.0000	6.9190	6.9830	0.0000	9.9915	0.0918	0.0000	4.9578	5.2556	0.0000
0.0894	9.4132	0.0000	6.9807	6.8694	0.0000	9.9952	0.0689	0.0000	4.8632	5.3519	0.0000
0.1020	9.4399	0.0000	7.0414	6.7557	0.0000	9.9979	0.0459	0.0000	4.7682	5.4472	0.0000
0.1157	9.4669	0.0000	7.1013	6.6420	0.0000	9.9995	0.0230	0.0000	4.6729	5.5414	0.0000
0.1306	9.4942	0.0000	7.1602	6.5282	0.0000	10.0000	0.0000	0.0000	4.5772	5.6343	0.0000
0.1468	9.5216	0.0000	7.2184	6.4144	0.0000	9.9993	-0.0265	0.0000	4.4813	5.7260	0.0000
0.1644	9.5493	0.0000	7.2756	6.3008	0.0000	9.9972	-0.0531	0.0000	4.3852	5.8163	0.0000
0.1834	9.5772	0.0000	7.3322	6.1873	0.0000	9.9936	-0.0796	0.0000	4.2890	5.9052	0.0000
0.2038	9.6050	0.0000	7.3879	6.0741	0.0000	9.9886	-0.1062	0.0000	4.1925	5.9927	0.0000
0.2258	9.6330	0.0000	7.4428	5.9611	0.0000	9.9821	-0.1326	0.0000	4.0960	6.0787	0.0000
0.2495	9.6608	0.0000	7.4971	5.8486	0.0000	9.9740	-0.1590	0.0000	3.9995	6.1632	0.0000
0.2749	9.6886	0.0000	7.5506	5.7364	0.0000	9.9644	-0.1853	0.0000	3.9030	6.2460	0.0000
0.3020	9.7162	0.0000	7.6034	5.6246	0.0000	9.9531	-0.2115	0.0000	3.8066	6.3272	0.0000
0.3310	9.7434	0.0000	7.6555	5.5134	0.0000	9.9401	-0.2374	0.0000	3.7102	6.4067	0.0000
0.3621	9.7699	0.0000	7.7070	5.4028	0.0000	9.9252	-0.2630	0.0000	3.6140	6.4844	0.0000
0.3952	9.7959	0.0000	7.7577	5.2927	0.0000	9.9086	-0.2883	0.0000	3.5180	6.5604	0.0000
0.4299	9.8217	0.0000	7.8078	5.1833	0.0000	9.8899	-0.3130	0.0000	3.4224	6.6346	0.0000
0.4660	9.8476	0.0000	7.8572	5.0746	0.0000	9.8692	-0.3372	0.0000	3.3270	6.7069	0.0000
0.5035	9.8738	0.0000	7.9060	4.9666	0.0000	9.8464	-0.3606	0.0000	3.2320	6.7773	0.0000
0.5423	9.9002	0.0000	7.9542	4.8594	0.0000	9.8214	-0.3830	0.0000	3.1374	6.8459	0.0000
0.5826	9.9267	0.0000	8.0017	4.7529	0.0000	9.7942	-0.4043	0.0000	3.0432	6.9125	0.0000
0.6243	9.9535	0.0000	8.0486	4.6474	0.0000	9.7647	-0.4242	0.0000	2.9496	6.9772	0.0000
0.6674	9.9805	0.0000	8.0949	4.5427	0.0000	9.7329	-0.4424	0.0000	2.8567	7.0399	0.0000
0.7120	10.0078	0.0000	8.1405	4.4390	0.0000	9.6988	-0.4588	0.0000	2.7643	7.1006	0.0000

0.7580	10.0353	0.0000	8.1856	4.3362	0.0000	9.6624	-0.4729	0.0000	2.6727	7.1594	0.0000
0.8055	10.0631	0.0000	8.2300	4.2344	0.0000	9.6239	-0.4844	0.0000	2.5818	7.2162	0.0000
0.8545	10.0911	0.0000	8.2738	4.1336	0.0000	9.5832	-0.4930	0.0000	2.4917	7.2710	0.0000
0.9049	10.1195	0.0000	8.3170	4.0340	0.0000	9.5406	-0.4984	0.0000	2.4024	7.3238	0.0000
0.9569	10.1480	0.0000	8.3596	3.9354	0.0000	9.4963	-0.5000	0.0000	2.3141	7.3746	0.0000
1.0105	10.1765	0.0000	8.4016	3.8378	0.0000	9.4506	-0.4976	0.0000	2.2267	7.4235	0.0000
1.0658	10.2051	0.0000	8.4430	3.7415	0.0000	9.4038	-0.4906	0.0000	2.1404	7.4704	0.0000
1.1227	10.2335	0.0000	8.4838	3.6463	0.0000	9.3566	-0.4789	0.0000	2.0551	7.5154	0.0000
1.1814	10.2618	0.0000	8.5240	3.5523	0.0000	9.3091	-0.4620	0.0000	1.9710	7.5584	0.0000
1.2420	10.2897	0.0000	8.5636	3.4596	0.0000	9.2619	-0.4398	0.0000	1.8880	7.5996	0.0000
1.3044	10.3173	0.0000	8.6026	3.3680	0.0000	9.2160	-0.4120	0.0000	1.8062	7.6389	0.0000
1.3686	10.3443	0.0000	8.6410	3.2777	0.0000	9.1724	-0.3780	0.0000	1.7256	7.6764	0.0000
1.4348	10.3707	0.0000	8.6788	3.1887	0.0000	9.1326	-0.3376	0.0000	1.6464	7.7120	0.0000
1.5028	10.3965	0.0000	8.7159	3.1010	0.0000	9.0958	-0.2918	0.0000	1.5684	7.7459	0.0000
1.5728	10.4214	0.0000	8.7526	3.0146	0.0000	9.0605	-0.2424	0.0000	1.4919	7.7781	0.0000
1.6447	10.4454	0.0000	8.7886	2.9296	0.0000	9.0256	-0.1907	0.0000	1.4167	7.8085	0.0000
1.7186	10.4682	0.0000	8.8240	2.8458	0.0000	8.9908	-0.1369	0.0000	1.3430	7.8374	0.0000
1.7945	10.4899	0.0000	8.8588	2.7635	0.0000	8.9560	-0.0810	0.0000	1.2708	7.8648	0.0000
1.8723	10.5101	0.0000	8.8930	2.6825	0.0000	8.9210	-0.0230	0.0000	1.2000	7.8908	0.0000
1.9521	10.5288	0.0000	8.9267	2.6028	0.0000	8.8855	0.0368	0.0000	1.1308	7.9153	0.0000
2.0338	10.5457	0.0000	8.9597	2.5246	0.0000	8.8492	0.0983	0.0000	1.0630	7.9381	0.0000
2.1174	10.5607	0.0000	8.9922	2.4478	0.0000	8.8117	0.1613	0.0000	0.9967	7.9591	0.0000
2.2030	10.5736	0.0000	9.0240	2.3723	0.0000	8.7726	0.2257	0.0000	0.9318	7.9785	0.0000
2.2903	10.5842	0.0000	9.0553	2.2983	0.0000	8.7320	0.2913	0.0000	0.8686	7.9968	0.0000
2.3794	10.5923	0.0000	9.0860	2.2256	0.0000	8.6898	0.3583	0.0000	0.8071	8.0146	0.0000
2.4702	10.5977	0.0000	9.1161	2.1544	0.0000	8.6461	0.4267	0.0000	0.7474	8.0322	0.0000
2.5626	10.6004	0.0000	9.1456	2.0846	0.0000	8.6011	0.4965	0.0000	0.6897	8.0502	0.0000
2.6565	10.6000	0.0000	9.1745	2.0162	0.0000	8.5549	0.5679	0.0000	0.6344	8.0696	0.0000
2.7518	10.5965	0.0000	9.2029	1.9493	0.0000	8.5077	0.6408	0.0000	0.5819	8.0914	0.0000
2.8483	10.5896	0.0000	9.2306	1.8837	0.0000	8.4594	0.7154	0.0000	0.5324	8.1159	0.0000
2.9460	10.5794	0.0000	9.2578	1.8196	0.0000	8.4102	0.7916	0.0000	0.4858	8.1423	0.0000
3.0445	10.5655	0.0000	9.2845	1.7568	0.0000	8.3598	0.8694	0.0000	0.4421	8.1702	0.0000
3.1439	10.5480	0.0000	9.3106	1.6955	0.0000	8.3083	0.9486	0.0000	0.4011	8.1993	0.0000
3.2440	10.5268	0.0000	9.3361	1.6355	0.0000	8.2556	1.0294	0.0000	0.3628	8.2293	0.0000
3.3446	10.5018	0.0000	9.3610	1.5770	0.0000	8.2016	1.1114	0.0000	0.3272	8.2602	0.0000
3.4454	10.4729	0.0000	9.3854	1.5198	0.0000	8.1464	1.1949	0.0000	0.2941	8.2917	0.0000
3.5465	10.4402	0.0000	9.4092	1.4639	0.0000	8.0899	1.2797	0.0000	0.2635	8.3236	0.0000
3.6476	10.4038	0.0000	9.4325	1.4094	0.0000	8.0322	1.3659	0.0000	0.2352	8.3558	0.0000
3.7486	10.3635	0.0000	9.4552	1.3562	0.0000	7.9734	1.4534	0.0000	0.2091	8.3880	0.0000
3.8494	10.3195	0.0000	9.4774	1.3044	0.0000	7.9133	1.5422	0.0000	0.1852	8.4203	0.0000
3.9497	10.2718	0.0000	9.4990	1.2538	0.0000	7.8521	1.6322	0.0000	0.1632	8.4524	0.0000
4.0496	10.2206	0.0000	9.5200	1.2045	0.0000	7.7897	1.7234	0.0000	0.1432	8.4844	0.0000
4.1489	10.1658	0.0000	9.5406	1.1565	0.0000	7.7261	1.8158	0.0000	0.1249	8.5161	0.0000

4.2475	10.1076	0.0000	9.5606	1.1097	0.0000	7.6613	1.9094	0.0000	0.1082	8.5474	0.0000
4.3453	10.0462	0.0000	9.5801	1.0642	0.0000	7.5954	2.0039	0.0000	0.0932	8.5784	0.0000
4.4423	9.9815	0.0000	9.5992	1.0199	0.0000	7.5283	2.0996	0.0000	0.0797	8.6090	0.0000
4.5385	9.9138	0.0000	9.6177	0.9768	0.0000	7.4600	2.1962	0.0000	0.0675	8.6392	0.0000
4.6336	9.8432	0.0000	9.6358	0.9348	0.0000	7.3906	2.2937	0.0000	0.0565	8.6690	0.0000
4.7278	9.7696	0.0000	9.6535	0.8941	0.0000	7.3201	2.3921	0.0000	0.0467	8.6984	0.0000
4.8210	9.6934	0.0000	9.6707	0.8544	0.0000	7.2485	2.4914	0.0000	0.0378	8.7273	0.0000
4.9132	9.6146	0.0000	9.6874	0.8158	0.0000	7.1757	2.5914	0.0000	0.0300	8.7558	0.0000
5.0042	9.5334	0.0000	9.7038	0.7784	0.0000	7.1019	2.6921	0.0000	0.0232	8.7840	0.0000
5.0942	9.4497	0.0000	9.7198	0.7420	0.0000	7.0270	2.7935	0.0000	0.0174	8.8118	0.0000
5.1831	9.3638	0.0000	9.7353	0.7066	0.0000	6.9510	2.8954	0.0000	0.0128	8.8393	0.0000
5.2709	9.2758	0.0000	9.7505	0.6722	0.0000	6.8739	2.9980	0.0000	0.0092	8.8665	0.0000
5.3576	9.1858	0.0000	9.7652	0.6388	0.0000	6.7958	3.1010	0.0000	0.0066	8.8936	0.0000
5.4432	9.0938	0.0000	9.7796	0.6062	0.0000	6.7168	3.2044	0.0000	0.0048	8.9204	0.0000
5.5277	9.0000	0.0000	9.7936	0.5746	0.0000	6.6366	3.3081	0.0000	0.0032	8.9470	0.0000
5.6110	8.9045	0.0000	9.8073	0.5438	0.0000	6.5556	3.4122	0.0000	0.0017	8.9736	0.0000
5.6932	8.8074	0.0000	9.8206	0.5139	0.0000	6.4736	3.5164	0.0000			

Boundary Points

x	y	z	x	y	x	x	y	z	x	y	z
0.0000	9.0000	0.0000	9.5801	1.0642	0.0000	0.4858	8.1423	0.0000	-0.7500	4.0000	0.0000
0.0011	9.0230	0.0000	9.5992	1.0199	0.0000	0.4421	8.1702	0.0000	-1.1250	4.0000	0.0000
0.0020	9.0460	0.0000	9.6177	0.9768	0.0000	0.4011	8.1993	0.0000	-1.5000	4.0000	0.0000
0.0031	9.0690	0.0000	9.6358	0.9348	0.0000	0.3628	8.2293	0.0000	-1.8750	4.0000	0.0000
0.0045	9.0922	0.0000	9.6535	0.8941	0.0000	0.3272	8.2602	0.0000	-2.2500	4.0000	0.0000
0.0066	9.1155	0.0000	9.6707	0.8544	0.0000	0.2941	8.2917	0.0000	-2.6250	4.0000	0.0000
0.0095	9.1390	0.0000	9.6874	0.8158	0.0000	0.2635	8.3236	0.0000	-3.0000	4.0000	0.0000
0.0131	9.1626	0.0000	9.7038	0.7784	0.0000	0.2352	8.3558	0.0000	-3.3750	4.0000	0.0000
0.0174	9.1864	0.0000	9.7198	0.7420	0.0000	0.2091	8.3880	0.0000	-3.7500	4.0000	0.0000
0.0224	9.2105	0.0000	9.7353	0.7066	0.0000	0.1852	8.4203	0.0000	-4.1250	4.0000	0.0000
0.0280	9.2348	0.0000	9.7505	0.6722	0.0000	0.1632	8.4524	0.0000	-4.5000	4.0000	0.0000
0.0343	9.2594	0.0000	9.7652	0.6388	0.0000	0.1432	8.4844	0.0000	-4.8750	4.0000	0.0000
0.0413	9.2842	0.0000	9.7796	0.6062	0.0000	0.1249	8.5161	0.0000	-5.2500	4.0000	0.0000
0.0491	9.3094	0.0000	9.7936	0.5746	0.0000	0.1082	8.5474	0.0000	-5.6250	4.0000	0.0000
0.0577	9.3349	0.0000	9.8073	0.5438	0.0000	0.0932	8.5784	0.0000	-6.0000	4.0000	0.0000
0.0673	9.3607	0.0000	9.8206	0.5139	0.0000	0.0797	8.6090	0.0000	-6.0000	4.3846	0.0000
0.0778	9.3868	0.0000	9.8335	0.4848	0.0000	0.0675	8.6392	0.0000	-6.0000	4.7692	0.0000
0.0894	9.4132	0.0000	9.8461	0.4564	0.0000	0.0565	8.6690	0.0000	-6.0000	5.1538	0.0000
0.1020	9.4399	0.0000	9.8583	0.4287	0.0000	0.0467	8.6984	0.0000	-6.0000	5.5385	0.0000
0.1157	9.4669	0.0000	9.8703	0.4017	0.0000	0.0378	8.7273	0.0000	-6.0000	5.9231	0.0000
0.1306	9.4942	0.0000	9.8819	0.3753	0.0000	0.0300	8.7558	0.0000	-6.0000	6.3077	0.0000
0.1468	9.5216	0.0000	9.8932	0.3496	0.0000	0.0232	8.7840	0.0000	-6.0000	6.6923	0.0000
0.1644	9.5493	0.0000	9.9042	0.3244	0.0000	0.0174	8.8118	0.0000	-6.0000	7.0769	0.0000
0.1834	9.5772	0.0000	9.9150	0.2998	0.0000	0.0128	8.8393	0.0000	-6.0000	7.4616	0.0000
0.2038	9.6050	0.0000	9.9256	0.2756	0.0000	0.0092	8.8665	0.0000	-6.0000	7.8462	0.0000
0.2258	9.6330	0.0000	9.9358	0.2519	0.0000	0.0066	8.8936	0.0000	-6.0000	8.2308	0.0000
0.2495	9.6608	0.0000	9.9459	0.2286	0.0000	0.0048	8.9204	0.0000	-6.0000	8.6154	0.0000
0.2749	9.6886	0.0000	9.9558	0.2057	0.0000	0.0032	8.9470	0.0000	-6.0000	9.0000	0.0000
0.3020	9.7162	0.0000	9.9653	0.1831	0.0000	17.5000	5.0000	0.0000	-6.0000	9.3846	0.0000
0.3310	9.7434	0.0000	9.9736	0.1604	0.0000	17.5000	4.6154	0.0000	-6.0000	9.7692	0.0000
0.3621	9.7699	0.0000	9.9807	0.1376	0.0000	17.5000	4.2308	0.0000	-6.0000	10.1538	0.0000
0.3952	9.7959	0.0000	9.9867	0.1147	0.0000	17.5000	3.8462	0.0000	-6.0000	10.5385	0.0000
0.4299	9.8217	0.0000	9.9915	0.0918	0.0000	17.5000	3.4616	0.0000	-6.0000	10.9231	0.0000
0.4660	9.8476	0.0000	9.9952	0.0689	0.0000	17.5000	3.0769	0.0000	-6.0000	11.3077	0.0000
0.5035	9.8738	0.0000	9.9979	0.0459	0.0000	17.5000	2.6923	0.0000	-6.0000	11.6923	0.0000
0.5423	9.9002	0.0000	9.9995	0.0230	0.0000	17.5000	2.3077	0.0000	-6.0000	12.0769	0.0000
0.5826	9.9267	0.0000	10.0000	0.0000	0.0000	17.5000	1.9231	0.0000	-6.0000	12.4616	0.0000
0.6243	9.9535	0.0000	9.9993	-0.0265	0.0000	17.5000	1.5385	0.0000	-6.0000	12.8462	0.0000
0.6674	9.9805	0.0000	9.9972	-0.0531	0.0000	17.5000	1.1538	0.0000	-6.0000	13.2308	0.0000
0.7120	10.0078	0.0000	9.9936	-0.0796	0.0000	17.5000	0.7692	0.0000	-6.0000	13.6154	0.0000
0.7580	10.0353	0.0000	9.9886	-0.1062	0.0000	17.5000	0.3846	0.0000	-6.0000	14.0000	0.0000
0.8055	10.0631	0.0000	9.9821	-0.1326	0.0000	17.5000	0.0000	0.0000	-5.6250	14.0000	0.0000
0.8545	10.0911	0.0000	9.9740	-0.1590	0.0000	17.5000	-0.3846	0.0000	-5.2500	14.0000	0.0000

0.9049	10.1195	0.0000	9.9644	-0.1853	0.0000	17.5000	-0.7692	0.0000	-4.8750	14.0000	0.0000
0.9569	10.1480	0.0000	9.9531	-0.2115	0.0000	17.5000	-1.1538	0.0000	-4.5000	14.0000	0.0000
1.0105	10.1765	0.0000	9.9401	-0.2374	0.0000	17.5000	-1.5385	0.0000	-4.1250	14.0000	0.0000
1.0658	10.2051	0.0000	9.9252	-0.2630	0.0000	17.5000	-1.9231	0.0000	-3.7500	14.0000	0.0000
1.1227	10.2335	0.0000	9.9086	-0.2883	0.0000	17.5000	-2.3077	0.0000	-3.3750	14.0000	0.0000
1.1814	10.2618	0.0000	9.8899	-0.3130	0.0000	17.5000	-2.6923	0.0000	-3.0000	14.0000	0.0000
1.2420	10.2897	0.0000	9.8692	-0.3372	0.0000	17.5000	-3.0769	0.0000	-2.6250	14.0000	0.0000
1.3044	10.3173	0.0000	9.8464	-0.3606	0.0000	17.5000	-3.4616	0.0000	-2.2500	14.0000	0.0000
1.3686	10.3443	0.0000	9.8214	-0.3830	0.0000	17.5000	-3.8462	0.0000	-1.8750	14.0000	0.0000
1.4348	10.3707	0.0000	9.7942	-0.4043	0.0000	17.5000	-4.2308	0.0000	-1.5000	14.0000	0.0000
1.5028	10.3965	0.0000	9.7647	-0.4242	0.0000	17.5000	-4.6154	0.0000	-1.1250	14.0000	0.0000
1.5728	10.4214	0.0000	9.7329	-0.4424	0.0000	17.5000	-5.0000	0.0000	-0.7500	14.0000	0.0000
1.6447	10.4454	0.0000	9.6988	-0.4588	0.0000	17.2500	-5.0000	0.0000	-0.3750	14.0000	0.0000
1.7186	10.4682	0.0000	9.6624	-0.4729	0.0000	17.0000	-5.0000	0.0000	0.0000	14.0000	0.0000
1.7945	10.4899	0.0000	9.6239	-0.4844	0.0000	16.7500	-5.0000	0.0000	0.1450	14.0001	0.0000
1.8723	10.5101	0.0000	9.5832	-0.4930	0.0000	16.5000	-5.0000	0.0000	0.2899	14.0002	0.0000
1.9521	10.5288	0.0000	9.5406	-0.4984	0.0000	16.2500	-5.0000	0.0000	0.4348	14.0003	0.0000
2.0338	10.5457	0.0000	9.4963	-0.5000	0.0000	16.0000	-5.0000	0.0000	0.5796	14.0088	0.0000
2.1174	10.5607	0.0000	9.4506	-0.4976	0.0000	15.7500	-5.0000	0.0000	0.7233	14.0271	0.0000
2.2030	10.5736	0.0000	9.4038	-0.4906	0.0000	15.5000	-5.0000	0.0000	0.8668	14.0477	0.0000
2.2903	10.5842	0.0000	9.3566	-0.4789	0.0000	15.2500	-5.0000	0.0000	1.0106	14.0656	0.0000
2.3794	10.5923	0.0000	9.3091	-0.4620	0.0000	15.0000	-5.0000	0.0000	1.1551	14.0780	0.0000
2.4702	10.5977	0.0000	9.2619	-0.4398	0.0000	14.7500	-5.0000	0.0000	1.2998	14.0846	0.0000
2.5626	10.6004	0.0000	9.2160	-0.4120	0.0000	14.5000	-5.0000	0.0000	1.4448	14.0859	0.0000
2.6565	10.6000	0.0000	9.1724	-0.3780	0.0000	14.2500	-5.0000	0.0000	1.5897	14.0818	0.0000
2.7518	10.5965	0.0000	9.1326	-0.3376	0.0000	14.0000	-5.0000	0.0000	1.7343	14.0725	0.0000
2.8483	10.5896	0.0000	9.0958	-0.2918	0.0000	13.7500	-5.0000	0.0000	1.8785	14.0578	0.0000
2.9460	10.5794	0.0000	9.0605	-0.2424	0.0000	13.5000	-5.0000	0.0000	2.0221	14.0377	0.0000
3.0445	10.5655	0.0000	9.0256	-0.1907	0.0000	13.2500	-5.0000	0.0000	2.1648	14.0126	0.0000
3.1439	10.5480	0.0000	8.9908	-0.1369	0.0000	13.0000	-5.0000	0.0000	2.3066	13.9823	0.0000
3.2440	10.5268	0.0000	8.9560	-0.0810	0.0000	12.7500	-5.0000	0.0000	2.4472	13.9469	0.0000
3.3446	10.5018	0.0000	8.9210	-0.0230	0.0000	12.5000	-5.0000	0.0000	2.5864	13.9067	0.0000
3.4454	10.4729	0.0000	8.8855	0.0368	0.0000	12.2500	-5.0000	0.0000	2.7242	13.8619	0.0000
3.5465	10.4402	0.0000	8.8492	0.0983	0.0000	12.0000	-5.0000	0.0000	2.8606	13.8126	0.0000
3.6476	10.4038	0.0000	8.8117	0.1613	0.0000	11.7500	-5.0000	0.0000	2.9952	13.7591	0.0000
3.7486	10.3635	0.0000	8.7726	0.2257	0.0000	11.5000	-5.0000	0.0000	3.1282	13.7014	0.0000
3.8494	10.3195	0.0000	8.7320	0.2913	0.0000	11.2500	-5.0000	0.0000	3.2595	13.6398	0.0000
3.9497	10.2718	0.0000	8.6898	0.3583	0.0000	11.0000	-5.0000	0.0000	3.3889	13.5746	0.0000

4.0496	10.2206	0.0000	8.6461	0.4267	0.0000	10.7500	-5.0000	0.0000	3.5164	13.5057	0.0000
4.1489	10.1658	0.0000	8.6011	0.4965	0.0000	10.5000	-5.0000	0.0000	3.6422	13.4336	0.0000
4.2475	10.1076	0.0000	8.5549	0.5679	0.0000	10.2500	-5.0000	0.0000	3.7660	13.3582	0.0000
4.3453	10.0462	0.0000	8.5077	0.6408	0.0000	10.0000	-5.0000	0.0000	3.8880	13.2799	0.0000
4.4423	9.9815	0.0000	8.4594	0.7154	0.0000	9.8612	-4.9645	0.0000	4.0081	13.1988	0.0000
4.5385	9.9138	0.0000	8.4102	0.7916	0.0000	9.7454	-4.8751	0.0000	4.1264	13.1150	0.0000
4.6336	9.8432	0.0000	8.3598	0.8694	0.0000	9.6394	-4.7769	0.0000	4.2428	13.0286	0.0000
4.7278	9.7696	0.0000	8.3083	0.9486	0.0000	9.5405	-4.6707	0.0000	4.3574	12.9400	0.0000
4.8210	9.6934	0.0000	8.2556	1.0294	0.0000	9.4466	-4.5604	0.0000	4.4703	12.8490	0.0000
4.9132	9.6146	0.0000	8.2016	1.1114	0.0000	9.3571	-4.4463	0.0000	4.5815	12.7560	0.0000
5.0042	9.5334	0.0000	8.1464	1.1949	0.0000	9.2719	-4.3290	0.0000	4.6910	12.6610	0.0000
5.0942	9.4497	0.0000	8.0899	1.2797	0.0000	9.1916	-4.2084	0.0000	4.7988	12.5641	0.0000
5.1831	9.3638	0.0000	8.0322	1.3659	0.0000	9.1175	-4.0838	0.0000	4.9050	12.4655	0.0000
5.2709	9.2758	0.0000	7.9734	1.4534	0.0000	9.0487	-3.9562	0.0000	5.0096	12.3652	0.0000
5.3576	9.1858	0.0000	7.9133	1.5422	0.0000	8.9829	-3.8270	0.0000	5.1127	12.2632	0.0000
5.4432	9.0938	0.0000	7.8521	1.6322	0.0000	8.9181	-3.6974	0.0000	5.2142	12.1598	0.0000
5.5277	9.0000	0.0000	7.7897	1.7234	0.0000	8.8539	-3.5674	0.0000	5.3143	12.0550	0.0000
5.6110	8.9045	0.0000	7.7261	1.8158	0.0000	8.7896	-3.4375	0.0000	5.4130	11.9488	0.0000
5.6932	8.8074	0.0000	7.6613	1.9094	0.0000	8.7245	-3.3080	0.0000	5.5103	11.8414	0.0000
5.7744	8.7087	0.0000	7.5954	2.0039	0.0000	8.6588	-3.1788	0.0000	5.6063	11.7328	0.0000
5.8545	8.6086	0.0000	7.5283	2.0996	0.0000	8.5927	-3.0498	0.0000	5.7010	11.6230	0.0000
5.9335	8.5072	0.0000	7.4600	2.1962	0.0000	8.5264	-2.9208	0.0000	5.7943	11.5121	0.0000
6.0115	8.4045	0.0000	7.3906	2.2937	0.0000	8.4601	-2.7920	0.0000	5.8864	11.4002	0.0000
6.0885	8.3007	0.0000	7.3201	2.3921	0.0000	8.3936	-2.6632	0.0000	5.9774	11.2873	0.0000
6.1644	8.1958	0.0000	7.2485	2.4914	0.0000	8.3269	-2.5345	0.0000	6.0672	11.1736	0.0000
6.2392	8.0897	0.0000	7.1757	2.5914	0.0000	8.2600	-2.4059	0.0000	6.1559	11.0589	0.0000
6.3129	7.9827	0.0000	7.1019	2.6921	0.0000	8.1926	-2.2776	0.0000	6.2435	10.9434	0.0000
6.3853	7.8747	0.0000	7.0270	2.7935	0.0000	8.1250	-2.1494	0.0000	6.3299	10.8270	0.0000
6.4564	7.7657	0.0000	6.9510	2.8954	0.0000	8.0570	-2.0214	0.0000	6.4150	10.7097	0.0000
6.5263	7.6559	0.0000	6.8739	2.9980	0.0000	7.9886	-1.8935	0.0000	6.4990	10.5915	0.0000
6.5948	7.5452	0.0000	6.7958	3.1010	0.0000	7.9199	-1.7659	0.0000	6.5817	10.4725	0.0000
6.6620	7.4338	0.0000	6.7168	3.2044	0.0000	7.8507	-1.6385	0.0000	6.6632	10.3526	0.0000
6.7278	7.3218	0.0000	6.6366	3.3081	0.0000	7.7812	-1.5114	0.0000	6.7435	10.2320	0.0000
6.7926	7.2092	0.0000	6.5556	3.4122	0.0000	7.7111	-1.3845	0.0000	6.8228	10.1106	0.0000
6.8563	7.0962	0.0000	6.4736	3.5164	0.0000	7.6406	-1.2578	0.0000	6.9010	9.9886	0.0000
6.9190	6.9830	0.0000	6.3906	3.6208	0.0000	7.5696	-1.1315	0.0000	6.9784	9.8660	0.0000
6.9807	6.8694	0.0000	6.3068	3.7254	0.0000	7.4980	-1.0054	0.0000	7.0549	9.7429	0.0000
7.0414	6.7557	0.0000	6.2220	3.8298	0.0000	7.4258	-0.8797	0.0000	7.1306	9.6193	0.0000

7.1013	6.6420	0.0000	6.1364	3.9343	0.0000	7.3530	-0.7544	0.0000	7.2054	9.4952	0.0000
7.1602	6.5282	0.0000	6.0500	4.0386	0.0000	7.2795	-0.6294	0.0000	7.2795	9.3706	0.0000
7.2184	6.4144	0.0000	5.9627	4.1428	0.0000	7.2054	-0.5049	0.0000	7.3530	9.2456	0.0000
7.2756	6.3008	0.0000	5.8747	4.2466	0.0000	7.1306	-0.3807	0.0000	7.4258	9.1203	0.0000
7.3322	6.1873	0.0000	5.7859	4.3502	0.0000	7.0549	-0.2571	0.0000	7.4980	8.9946	0.0000
7.3879	6.0741	0.0000	5.6964	4.4533	0.0000	6.9784	-0.1340	0.0000	7.5696	8.8686	0.0000
7.4428	5.9611	0.0000	5.6061	4.5560	0.0000	6.9010	-0.0114	0.0000	7.6406	8.7422	0.0000
7.4971	5.8486	0.0000	5.5152	4.6581	0.0000	6.8228	0.1106	0.0000	7.7111	8.6156	0.0000
7.5506	5.7364	0.0000	5.4237	4.7596	0.0000	6.7435	0.2320	0.0000	7.7812	8.4886	0.0000
7.6034	5.6246	0.0000	5.3316	4.8604	0.0000	6.6632	0.3526	0.0000	7.8507	8.3615	0.0000
7.6555	5.5134	0.0000	5.2389	4.9605	0.0000	6.5817	0.4725	0.0000	7.9199	8.2341	0.0000
7.7070	5.4028	0.0000	5.1457	5.0598	0.0000	6.4990	0.5915	0.0000	7.9886	8.1065	0.0000
7.7577	5.2927	0.0000	5.0520	5.1581	0.0000	6.4150	0.7097	0.0000	8.0570	7.9787	0.0000
7.8078	5.1833	0.0000	4.9578	5.2556	0.0000	6.3299	0.8270	0.0000	8.1250	7.8506	0.0000
7.8572	5.0746	0.0000	4.8632	5.3519	0.0000	6.2435	0.9434	0.0000	8.1926	7.7225	0.0000
7.9060	4.9666	0.0000	4.7682	5.4472	0.0000	6.1559	1.0589	0.0000	8.2600	7.5941	0.0000
7.9542	4.8594	0.0000	4.6729	5.5414	0.0000	6.0672	1.1736	0.0000	8.3269	7.4655	0.0000
8.0017	4.7529	0.0000	4.5772	5.6343	0.0000	5.9774	1.2874	0.0000	8.3936	7.3368	0.0000
8.0486	4.6474	0.0000	4.4813	5.7260	0.0000	5.8864	1.4002	0.0000	8.4601	7.2080	0.0000
8.0949	4.5427	0.0000	4.3852	5.8163	0.0000	5.7943	1.5121	0.0000	8.5264	7.0792	0.0000
8.1405	4.4390	0.0000	4.2890	5.9052	0.0000	5.7010	1.6230	0.0000	8.5927	6.9502	0.0000
8.1856	4.3362	0.0000	4.1925	5.9927	0.0000	5.6063	1.7328	0.0000	8.6588	6.8212	0.0000
8.2300	4.2344	0.0000	4.0960	6.0787	0.0000	5.5103	1.8414	0.0000	8.7245	6.6920	0.0000
8.2738	4.1336	0.0000	3.9995	6.1632	0.0000	5.4130	1.9488	0.0000	8.7896	6.5625	0.0000
8.3170	4.0340	0.0000	3.9030	6.2460	0.0000	5.3143	2.0550	0.0000	8.8539	6.4326	0.0000
8.3596	3.9354	0.0000	3.8066	6.3272	0.0000	5.2142	2.1598	0.0000	8.9181	6.3026	0.0000
8.4016	3.8378	0.0000	3.7102	6.4067	0.0000	5.1127	2.2632	0.0000	8.9829	6.1730	0.0000
8.4430	3.7415	0.0000	3.6140	6.4844	0.0000	5.0096	2.3652	0.0000	9.0487	6.0438	0.0000
8.4838	3.6463	0.0000	3.5180	6.5604	0.0000	4.9050	2.4655	0.0000	9.1175	5.9163	0.0000
8.5240	3.5523	0.0000	3.4224	6.6346	0.0000	4.7988	2.5641	0.0000	9.1916	5.7916	0.0000
8.5636	3.4596	0.0000	3.3270	6.7069	0.0000	4.6910	2.6610	0.0000	9.2719	5.6710	0.0000
8.6026	3.3680	0.0000	3.2320	6.7773	0.0000	4.5815	2.7560	0.0000	9.3571	5.5537	0.0000
8.6410	3.2777	0.0000	3.1374	6.8459	0.0000	4.4703	2.8490	0.0000	9.4466	5.4396	0.0000
8.6788	3.1887	0.0000	3.0432	6.9125	0.0000	4.3574	2.9400	0.0000	9.5405	5.3293	0.0000
8.7159	3.1010	0.0000	2.9496	6.9772	0.0000	4.2428	3.0286	0.0000	9.6394	5.2231	0.0000
8.7526	3.0146	0.0000	2.8567	7.0399	0.0000	4.1264	3.1150	0.0000	9.7454	5.1249	0.0000
8.7886	2.9296	0.0000	2.7643	7.1006	0.0000	4.0081	3.1988	0.0000	9.8612	5.0356	0.0000
8.8240	2.8458	0.0000	2.6727	7.1594	0.0000	3.8880	3.2799	0.0000	10.0000	5.0000	0.0000
8.8588	2.7635	0.0000	2.5818	7.2162	0.0000	3.7660	3.3582	0.0000	10.2500	5.0000	0.0000
8.8930	2.6825	0.0000	2.4917	7.2710	0.0000	3.6422	3.4336	0.0000	10.5000	5.0000	0.0000
8.9267	2.6028	0.0000	2.4024	7.3238	0.0000	3.5164	3.5057	0.0000	10.7500	5.0000	0.0000
8.9597	2.5246	0.0000	2.3141	7.3746	0.0000	3.3889	3.5746	0.0000	11.0000	5.0000	0.0000
8.9922	2.4478	0.0000	2.2267	7.4235	0.0000	3.2595	3.6398	0.0000	11.2500	5.0000	0.0000
9.0240	2.3723	0.0000	2.1404	7.4704	0.0000	3.1282	3.7014	0.0000	11.5000	5.0000	0.0000
9.0553	2.2983	0.0000	2.0551	7.5154	0.0000	2.9952	3.7591	0.0000	11.7500	5.0000	0.0000
9.0860	2.2256	0.0000	1.9710	7.5584	0.0000	2.8606	3.8126	0.0000	12.0000	5.0000	0.0000

9.1161	2.1544	0.0000	1.8880	7.5996	0.0000	2.7242	3.8619	0.0000	12.2500	5.0000	0.0000
9.1456	2.0846	0.0000	1.8062	7.6389	0.0000	2.5864	3.9067	0.0000	12.5000	5.0000	0.0000
9.1745	2.0162	0.0000	1.7256	7.6764	0.0000	2.4472	3.9469	0.0000	12.7500	5.0000	0.0000
9.2029	1.9493	0.0000	1.6464	7.7120	0.0000	2.3066	3.9823	0.0000	13.0000	5.0000	0.0000
9.2306	1.8837	0.0000	1.5684	7.7459	0.0000	2.1648	4.0126	0.0000	13.2500	5.0000	0.0000
9.2578	1.8196	0.0000	1.4919	7.7781	0.0000	2.0221	4.0377	0.0000	13.5000	5.0000	0.0000
9.2845	1.7568	0.0000	1.4167	7.8085	0.0000	1.8785	4.0578	0.0000	13.7500	5.0000	0.0000
9.3106	1.6955	0.0000	1.3430	7.8374	0.0000	1.7343	4.0725	0.0000	14.0000	5.0000	0.0000
9.3361	1.6355	0.0000	1.2708	7.8648	0.0000	1.5897	4.0818	0.0000	14.2500	5.0000	0.0000
9.3610	1.5770	0.0000	1.2000	7.8908	0.0000	1.4448	4.0859	0.0000	14.5000	5.0000	0.0000
9.3854	1.5198	0.0000	1.1308	7.9153	0.0000	1.2998	4.0846	0.0000	14.7500	5.0000	0.0000
9.4092	1.4639	0.0000	1.0630	7.9381	0.0000	1.1551	4.0780	0.0000	15.0000	5.0000	0.0000
9.4325	1.4094	0.0000	0.9967	7.9591	0.0000	1.0106	4.0656	0.0000	15.2500	5.0000	0.0000
9.4552	1.3562	0.0000	0.9318	7.9785	0.0000	0.8668	4.0477	0.0000	15.5000	5.0000	0.0000
9.4774	1.3044	0.0000	0.8686	7.9968	0.0000	0.7233	4.0271	0.0000	15.7500	5.0000	0.0000
9.4990	1.2538	0.0000	0.8071	8.0146	0.0000	0.5796	4.0088	0.0000	16.0000	5.0000	0.0000
9.5200	1.2045	0.0000	0.7474	8.0322	0.0000	0.4348	4.0003	0.0000	16.2500	5.0000	0.0000
9.5406	1.1565	0.0000	0.6897	8.0502	0.0000	0.2899	4.0002	0.0000	16.5000	5.0000	0.0000
9.5606	1.1097	0.0000	0.6344	8.0696	0.0000	0.1450	4.0001	0.0000	16.7500	5.0000	0.0000
			0.5819	8.0914	0.0000	0.0000	4.0000	0.0000	17.0000	5.0000	0.0000
			0.5324	8.1159	0.0000	-0.3750	4.0000	0.0000	17.2500	5.0000	0.0000

```
!This FORTRAN 90 program generates a GAMBIT journal file used to run an automatic GAMBIT
!session using number of cooling holes (NCH) and number of data points per cooling hole
(NCHP).
!These two values are read from the first line of holepoints.dat and data in output to
gambitjournal.jou

program journalfilegenerator
implicit none
integer::i,j,k,vcount,NAP,NCH,NCHP,start,finish,Nedges,ecount,vecount,facecount,volumeco
unt
integer::Nfaces,Nvolumes,frontface,rearface,frontedge,rearedge,boundary
open(unit=2, file="gambitjournal.jou")
open(unit=3, file="holepoints.dat")

!Required values
!Read number of points per cooling hole (non-constant) number of cooling holes (non-
constant)
read (3,9) NCHP, NCH
9 format (I2,1x,I2)
!Number of Airfoil Points = 399 (constant)
NAP=399

!Initialize edge counter
Nedges=0
!Number of 2D faces = number of cooling holes + 1
Nfaces=NCH+1
Nvolumes=NCH+1

!Read 3D coordinates of airfoil and cooling holes points
!input file path for airfoil and cooling hole data points
!Airfoil data points are constant and hole data points are provided by the optimization
code
write (2,11) "import iceminput \",'"airfoilpoints.dat" \',"vertex"
write (2,11) "import iceminput \",'"holepoints.dat" \',"vertex"
!write (2,11) "import iceminput \",'"C:\\Documents and
Settings\\Owner\\Desktop\\Fortran\\airfoilpoints.dat" \',"vertex"
!write (2,11) "import iceminput \",'"C:\\Documents and
Settings\\Owner\\Desktop\\Fortran\\holepoints.dat" \',"vertex"
11 format (A,/,2x,A,/,2x,A)

!Generates edges through the nurbs function for 40 points per instance
vcount=1
!count groups of nurbs
do k=1,NAP;
  write (2,13) "edge create nurbs \"
13 format (A)
Nedges=Nedges+1

!count lines
do j=1,7;
!count entries per line
do i=1,6;
  if (vcount.lt.10) then
       write (unit=2,fmt=15,advance="NO") '"vertex.',vcount,'"'
       15 format (2x,A,I1,A)
  elseif (vcount.lt.100) then
       write (unit=2,fmt=17,advance="NO") '"vertex.',vcount,'"'
    17 format (2x,A,I2,A)
  else
    write (unit=2,fmt=19,advance="NO") '"vertex.',vcount,'"'
    19 format (2x,A,I3,A)
  endif
  if (vcount.eq.(40*k)) then
    write (2,*) "interpolate"
    go to 14
  elseif (vcount.eq.NAP) then
```

```
       write (2,*) "interpolate"
       go to 16
  endif
  vcount=vcount+1
enddo
write (2,*) "\"
14 enddo
enddo

16 write (2,21) 'edge create nurbs "vertex.1" "vertex.',NAP,'" interpolate'
Nedges=Nedges+1
21 format (A,I3,A)

!generate the edges through the nurbs function for cooling holes
do i=1, NCH;
  write (2,13) "edge create nurbs \"
  Nedges=Nedges+1
  start=NAP+NCHP*(i-1)+1
  vcount=start
  finish=NAP+NCHP*i
do
do j=1,6;
       write (unit=2,fmt=19,advance="NO") '"vertex.',vcount,'"'
    if (vcount.eq.finish) then
    write (2,*) "interpolate"
       write (2,23) 'edge create nurbs "vertex.',start,'" "vertex.',finish,'"
interpolate'
    Nedges=Nedges+1
       23 format (A,I3,A,I3,A)
    go to 18
    endif
    vcount=vcount+1
enddo
       write (2,*) "\"
enddo
18 enddo

!merge edges created by nurbs
!merge first 11 edges to create airfoil edge
!merge following pair of edges up to Nedges to create cooling holes edges
ecount=1
vecount=0
write (2,13) "edge merge \"
vecount=vecount+1
do
do j=1,6;
    if (ecount.lt.10) then
    write (unit=2,fmt=15,advance="NO") '"edge.',ecount,'"'
    elseif (ecount.lt.11) then
    write (unit=2,fmt=17,advance="NO") '"edge.',ecount,'"'
       elseif (ecount.eq.11) then
    write (2,25) ' "edge.',ecount,'" forced'
       25 format (A,I2,A)
       go to 20
       endif
    ecount=ecount+1
enddo
write (2,*) "\"
enddo

20 do i=12,Nedges,2;
       write (unit=2,fmt=27) 'edge merge "edge.',i,'" "edge.',i+1,'" forced'
       27 format (A,I2,A,I2,A)
    vecount=vecount+1
enddo

!delete all vertices not associates with edges
!convert virtual edges to real edges
```

```
write (2,13) "vertex delete"
write (2,13) "edge convert"

!Increase edge count from conversion of virtual edges to real edges
Nedges=Nedges+1 !airfoil (72)
frontedge=Nedges
Nedges=Nedges+NCH !cooling holes (102)
rearedge=Nedges+1

!create airfoil and cooling hole faces (1-31) from edges (72-102)
facecount=0
do i=(Nedges-NCH),Nedges;
    if (i.lt.100)then
       write (2,29) 'face create wireframe "edge.',i,'" real'
    facecount=facecount+1
       29 format (A,I2,A)
    else if (i.lt.1000)then
    write (2,31) 'face create wireframe "edge.',i,'" real'
    facecount=facecount+1
       31 format (A,I3,A)
    endif
enddo

!Creates airfoil and cooling hole volumes from faces
write (2,13) 'volume create translate \'
facecount=1
do
  do i=1,6;
    if (facecount.lt.10) then
       write (unit=2,fmt=15,advance="NO") '"face.',facecount,'"'
       elseif (facecount.lt.100) then
    write (unit=2,fmt=17,advance="NO") '"face.',facecount,'"'
    endif
    if (facecount.eq.Nfaces) then
   go to 24
    endif
    facecount=facecount+1
  end do
write (2,*) "\"
enddo
24 write (2,13) " vector 0 0 -10"

!Update number of edges from volume creation
frontface=1
rearface=Nfaces+1 !rearface=32
boundary=Nfaces+2
Nedges=Nedges+(NCH+1)*2
Nfaces=3*(1+NCH) !93

!Subtract cooling hole volumes from airfoil volume
write (2,13) 'volume subtract "volume.1" volumes \'
volumecount=2
do
  do i=1,6;
    if (volumecount.lt.10) then
       write (unit=2,fmt=15,advance="NO") '"volume.',volumecount,'"'
       elseif (facecount.lt.100) then
    write (unit=2,fmt=17,advance="NO") '"volume.',volumecount,'"'
    endif
    if (volumecount.eq.Nvolumes) then
   go to 26
    endif
    volumecount=volumecount+1
  end do
write (2,*) "\"
enddo

!Update edgecount from subtraction of volumes
```

```
Nedges=Nedges+NCH*2
26 continue

!Mesh outer airfoil edge with 400 count (Nedges=102)
write (2,33) 'edge mesh "edge.',frontedge,'" successive ratio1 1 intervals 400'
33 format (/,A,I2,A)
if (rearedge.lt.100) then
write (2,99) 'edge mesh "edge.',rearedge,'" successive ratio1 1 intervals 400'
99 format (A,I2,A)
  else
write (2,35) 'edge mesh "edge.',rearedge,'" successive ratio1 1 intervals 400'
35 format (A,I3,A)
endif

!Mesh cooling hole edges with 30 count
start=Nedges+1
finish=Nedges+NCH*2
write (2,13) "edge mesh \"
do
 do i=1,6;
 if (start.lt.100) then
 write (unit=2,fmt=17,advance="NO") '"edge.',start,'"'
 else
 write (unit=2,fmt=19,advance="NO") '"edge.',start,'"'
 endif
 if (start.eq.finish) then
 go to 28
 endif
 start=start+1
 end do
 write (2,*) "\"
end do

28 write (2,*) "\"
write (2,13) "  successive ratio1 1 intervals 30"

!create boundary layer around cooling holes
write (2,37) "blayer create first 0.002 growth 1.5 total 1.0 rows 5 transition 1
\","trows 0"
37 format (A,/,2x,A)
write (2,13) 'blayer attach "b_layer.1" face \'
facecount=1
do
do i=1,6;
  write (unit=2,fmt=13,advance="NO") ' "face.1"'
  if (facecount.eq.NCH) then
    go to 30
  endif
  facecount=facecount+1
end do
write (2,*) "\"
end do

30 write (2,*) "\"
start=Nedges+2
finish=Nedges+(2*NCH)
write (2,13) "edge \"
do
 do i=1,6;
 if (start.lt.100) then
 write (unit=2,fmt=17,advance="NO") '"edge.',start,'"'
 else
 write (unit=2,fmt=19,advance="NO") '"edge.',start,'"'
 endif
 if (start.eq.finish) then
 go to 32
 endif
 start=start+2
```

```
 end do
 write (2,*) "\"
end do
32 write (2,*) "add"

!Generate face mesh
write (2,13) 'face mesh "face.1" triangle size 1'

!Generate volume mesh
if (rearface.lt.10) then
write (2,93) 'volume mesh "volume.1" cooper source "face.',rearface,'" "face.1" size 1'
93 format (A,I1,A)
elseif (rearface.lt.100) then
write (2,95) 'volume mesh "volume.1" cooper source "face.',rearface,'" "face.1" size 1'
95 format (A,I2,A)
else
write (2,97) 'volume mesh "volume.1" cooper source "face.',rearface,'" "face.1" size 1'
97 format (A,I3,A)
endif

!specify wall and material types
write (2,39) 'physics create "airfoil_front_wall" btype "WALL" face
"face.',frontface,'"'
  39 format (A,I1,A)
if (rearface.lt.100) then
  write (2,41) 'physics create "airfoil_rear_wall" btype "WALL" face
"face.',rearface,'"'
  41 format (A,I2,A)
else
  write (2,43) 'physics create "airfoil_rear_wall" btype "WALL" face
"face.',rearface,'"'
  43 format (A,I3,A)
endif
if (boundary.lt.100) then
  write (2,41) 'physics create "airfoil_interface" btype "WALL" face
"face.',boundary,'"'
else
  write (2,43) 'physics create "airfoil_interface" btype "WALL" face
"face.',boundary,'"'
endif
write (2,13) 'physics create "cooling_holes" btype "WALL" face \'
start=Nfaces-(2*NCH)+2
finish=Nfaces
do
  do i=1,6;
  if (start.eq.22) then
    go to 34
  end if
  if (start.lt.10) then
  write (unit=2,fmt=15,advance="NO") '"face.',start,'"'
  elseif (start.lt.100) then
  write (unit=2,fmt=17,advance="NO") '"face.',start,'"'
  endif
  if (start.eq.finish) then
  go to 36
  endif
  34 start=start+2
end do
write (2,*) "\"
end do
36 write (2,45) 'physics create "nickel" ctype "SOLID" volume "volume.1"'
45 format (/,A)
write (2,13) 'save name "airfoil.dbs"'
write (2,13) 'export fluent5 "airfoil.msh"'
stop
endprogram journalfilegenerator
```

```
;Always use the following line, otherwise the process may hang
/file/confirm-overwrite
no
;Read airfoil mesh file
/file/read-case
"airfoil.msh"
;Scale airfoil mesh file
/grid/scale
0.005
0.005
0.005
;Append airfoil mesh with boundary mesh
/grid/modify-zones/append-mesh-data
"boundary.cas"
;Define pressure units (atm)
/define/units
pressure
atm
;Interpolate unser-defined functions
/define/user-defined/interpreted-functions
"UDF.c"
"cc -E"
10000
yes
;Define solver
/define/models/solver/density-based-implicit
yes
;Enable energy equation
/define/models/energy
yes
;Define viscous model
/define/models/viscous/ke-realizable
yes
;Leave default Near-Wall-Treatment at Standard Wall Functions
;Add nickel to material list
/define/materials/copy
solid
nickel
;Change airfoil to nickel
/define/boundary-conditions/solid
nickel
yes
nickel
no
yes
0
0
0
0
0
1
no
;Rename airfoil default interior
/define/boundary-conditions/zone-name
default-interior
airfoil_mesh
;Change interface boundary types
/define/boundary-conditions/zone-type
```

```
airfoil_interface
interface
/define/boundary-conditions/zone-type
boundary_interface
interface
;Change remaining boundary types
/define/boundary-conditions/zone-type
boundary_front_wall
symmetry
/define/boundary-conditions/zone-type
boundary_rear_wall
symmetry
/define/boundary-conditions/zone-type
airfoil_front_wall
symmetry
/define/boundary-conditions/zone-type
airfoil_rear_wall
symmetry
;Define cooling hole boundary conditions
/define/boundary-conditions/wall
cooling_holes
0
no
0
no
yes
convection
no
994.96
yes
yes
"udf"
"z_temperature"
no
;Define grid interfaces by name
/define/grid-interfaces/create
interface
boundary_interface
()
airfoil_interface
()
no
yes
;Set Courant Number (CN)
/solve/set/courant-number
1
;Set flow discretization scheme to First Order Upwind
/solve/set/discretization-scheme/amg-c
0
;Initialize all zones
/solve/initialize/initialize-flow
;Write case file
/file/write-case
"fluent.cas"
;Exit Fluent
exit
yes
```

User Defined Function

```
/*********************************************
 UDF for specifying the temperature distribution
 along the -z direction of the turbine vane
 cooling holes.
 *********************************************/
#include "udf.h" /*must be at the beginning of every UDF written.*/
/*#include <math.h>*/

DEFINE_PROFILE(z_temperature,thread,index)
/* z-temperature=variable to be set, thread = surface to apply bc to
(boundary zone), index=defined automatically */
{
real x[ND_ND];  /*this holds a position vector for each face
centroid*/
real z;         /*this holds a position for the variable z*/
face_t f;
#if !RP_HOST
begin_f_loop(f,thread)
/*loops over all faces in the thread passed in the define macro
argument*/
 {
 F_CENTROID(x,f,thread); /*accesses the coordinates of the face
centroids along the length of the cooling hole*/
 z=x[2];                 /* assuming x=x[0], y=x[1], z=x[2] */
 F_PROFILE(f,thread,index) = 298.15+57.9*sqrt(fabs(z/5.0));
 }
end_f_loop(f,thread)
#endif
}
```

Parallel Fluent Input

```
;Always use the following line, otherwise the process may hang
/file/confirm-overwrite
no
;Read case file
/file/read-case
fluent.cas
;Initialize the solution
/solve/initialize/initialize-flow
;Set Courant Number
/solve/set/courant-number
2
;Iterate
it 200
;Increase Courant Number
/solve/set/courant-number
5
;Iterate
it 200
;Increase Courant Number
/solve/set/courant-number
7
;Iterate
it 600
;Report static temperature on airfoil interface
/plot/plot
yes
temperature
no
yes
1
0
0
no
no
temperature
airfoil_interface
()
;Report heat flux through airfoil interface (face 17 in this setup)
/report/fluxes/heat-transfer
no
17
()
yes
fluxes.flp
;Write data file
/file/write-data
fluent.dat
;Exit Fluent
exit
yes
```

Batch Script

```
#!/bin/csh
#  Batch file for running FLUENT jobs
#  start in the directory where the job was
#  submitted
#$ -cwd
#
#  total number of nodes requested(each node
#  has 2 processors)
#$ -l qty.eq.3
#
#  name of the job
#$ -N JAMESJOB
#
# commands to be executed
#call parallel Fluent using 'parafluent' script.
#Options can be added in quotes.
#To run a 3D simulation interactively using the GUI on 192.168.0.108,
    #type:
#parafluent "3ddp -cx 192.168.0.108:32795:32796"
#To run a 3D simulation in batch using the input journal file
    'flinput':
rm -rf holepoints.dat tec.dat
./interpreter airfoil.dat vars.txt
rm -rf gambitjournal.jou
./journalfilegenerator.exe
rm -rf airfoil.dbs airfoil.msh airfoil.jou airfoil.trn
time /usr/local/Fluent.Inc/bin/gambit -id airfoil -inp
    gambitjournal.jou
rm -rf fluent.cas
time /usr/local/Fluent.Inc/bin/fluent "3ddp -g -i fluentjournal"
rm -rf fluxes.flp temperature fluent.dat
time parafluent "3ddp -g -i parafluentinput"
./protemp
rm -rf object.obj
./outputfilegenerator.exe
```

Output File Generator

```
!This Fortran program generates the object(.obj)
!file that contains the heat flux over the airfoil
!and maximum temperature in the airfoil.
program outputgenerator
implicit none
real::flux,T,Tmax,junk
integer::i,n
character*128 c
open(unit=2,file="object.obj")
open(unit=3,file="fluxes.flp")
open(unit=4,file="temperature")

read (3,11) flux
11 format (4/,T40,F13.3)

Tmax=0

read (4,*) n
do i=1,n;
   read (4,*) T, junk
   if (T.gt.Tmax) then
     Tmax=T
   endif
enddo

write (2,17) flux,Tmax
17 format (F13.3,/,F13.3)

close (2)
close (3)
close (4)

stop
endprogram outputgenerator
```

90
0.00139658068
0.00106650883
0.206520546
0.00128796051
0.0128575897
0.184191067
0.00141686514
0.0294344477
0.207647725
0.00131965945
0.0528044866
0.161818009
0.00129742241
0.0812047564
0.217392751
0.00120929728
0.118242711
0.133556879
0.00133237903
0.163653777
0.183722364
0.00133252576
0.216317229
0.161924939
0.00121584981
0.270402209
0.199576069
0.00124362191
0.326459408
0.17198617
0.001341099
0.379200603
0.224909717
0.00128803036
0.425364755
0.169871239
0.00124598687
0.467241011
0.161479809
0.00128771389
0.491415928
0.157913729
0.00130338572
0.51457532
0.112631364
.....
.....
0.00116181054
0.530237202
0.0574039102
0.00129157242
0.542185853
0.0581244647
0.00125088702
0.554977382
0.0537588986
0.00120045181
0.571101345
0.0976948408
0.00120077566
0.593360724
0.218375738
0.00117617638
0.631119312
0.163186115
0.00132474057
0.671405475
0.158857738
0.00131841919
0.723955966
0.186763545
0.00130508261
0.770399942
0.174848964
0.00130642453
0.820597056
0.178451705
0.00117595784
0.870726629
0.145085894
0.0012187558
0.915034651
0.227090007
0.00122443973
0.944954229
0.17894446
0.00134757763
0.971907263
0.200739719
0.00131789401
0.98712133
0.160309259

REFERENCES

[1]. B.H. Dennis, G.S. Dulikravich, I.N. Igorov, S.Yochimura. “Optimization of a Large number of Coolant Passages Located close to the surface of a Turbine Blade”.

[2]. J.Tu, G.H.Yeoh, C. Liu, “COMPUTATIONAL FLUID DYNAMICS: A Practical Approach”, *Butterworth-Heinemann, Burlington, Massachusetts, 2008.*

[3]. T. Arts, M. Lambert de Rouvroit, A.W. Rutherford, “AERO-THERMAL INVESTIGATION OF A HIGHLY LOADED TRANSONIC LINEAR TURBINE GUIDE VANE CASCADE”, von Karman Institute for Fluid Dynamics Chaussee de Waterloo, Technical Note 147, September 1990.

[4]. G. Nowak, W. Wroblewski, “COOLING SYSTEM OPTIMISATION OF TURBINE GUIDE VANE”, Silesian University of Technology, Institute of Power Engineering and Turbomachinery.

[5]. H.K Versteeg, W. Malalaskera, “An Introduction to Computational Fluid Dynamics: The Finite Volume Method”, John Wiley & Sons, New York, 1995.

[6] K. Deb, “Multi-Objective Optimization using Evolutionary Algorithms”, John Wiley & Sons, New York, 2003.

[7]. L.D. Hylton, M.S. Mihelc, E.R. Turner, D.A. Nealy, R.E. York, “Analytical and Experimental Evaluation of Heat Transfer Distribution Over the Surface of Turbine Vanes”,NASA Lewis Research Center, NASA CR 168015, May 1983

[8]. “Fluent 6.3 User’s Guide”,Fluent Inc., September 2006

BIOGRAPHICAL INFORMATION

James' professional career started with his enlistment into the United States Air Force. While serving in the military, James trained as an Aircraft Mechanic working on F-16 Fighter Aircraft from 1995 to 1999.

At the end of his military career, in the Fall of 1999, James returned to Texas A&M University-College Station where he Graduated in 2003 with his Bachelor of Science degree in Aerospace Engineering. James then moved to Dallas, TX to work as a Project Engineer in the Automotive Industry. Shortly after moving to Dallas, in the Fall of 2005, James began his part-time Graduate studies at the University of Texas at Arlington where he studied under Dr. Brian Dennis is the field of Computational Fluid Dynamics (CFD). James' primary studies included CFD analysis and thermal design optimization on axial flow turbine blades. In the Summer of 2008, James began working for a CFD software company as an Applications Engineer. The following Fall, James graduated with his Master of Science Degree in Aerospace Engineering.

James continues to work in the field of CFD where he specializes in the Aerospace and Defense Sector. James aspires to continue his education in the field of CFD while focusing on applications of CFD in the Aerospace Industry.